

ISTANBUL TECHNICAL UNIVERSITY ★ ENERGY INSTITUTE

**CFD BASED THERMAL AND HYDRAULIC PERFORMANCE
INVESTIGATION OF AIR HEATING PLATE TYPE
SOLAR COLLECTORS WITH DIFFERENT DUCT PROFILES**

M.Sc. THESIS

Cem ÇORAPÇIOĞLU

Energy Science and Technology Division

Energy Science and Technology Programme

DECEMBER 2015

ISTANBUL TECHNICAL UNIVERSITY ★ ENERGY INSTITUTE

**CFD BASED THERMAL AND HYDRAULIC PERFORMANCE
INVESTIGATION OF AIR HEATING PLATE TYPE
SOLAR COLLECTORS WITH DIFFERENT DUCT PROFILES**

M.Sc. THESIS

**Cem ÇORAPÇIOĞLU
301121039**

Energy Science and Technology Division

Energy Science and Technology Programme

Thesis Advisor: Prof. Dr. Figen KADIRGAN

DECEMBER 2015

İSTANBUL TEKNİK ÜNİVERSİTESİ ★ ENERJİ ENSTİTÜSÜ

**FARKLI KANAL KESİTLERİNE SAHİP HAVA ISITICI
GÜNEŞ KOLEKTÖRLERİNİN CFD YÖNTEMİ İLE
ISIL VE HİDROLİK PERFORMANSLARININ İNCELENMESİ**

YÜKSEK LİSANS TEZİ

**Cem ÇORAPÇIOĞLU
301121039**

Enerji Bilim ve Teknoloji Anabilim Dalı

Enerji Bilim ve Teknoloji Programı

Tez Danışmanı: Prof. Dr. Figen KADIRGAN

ARALIK 2015

Cem ÇORAPÇIOĞLU, a M.Sc. student of ITU Institute of Energy student ID 301121039, successfully defended the thesis entitled “CFD BASED THERMAL AND HYDRAULIC PERFORMANCE INVESTIGATION OF AIR HEATINGPLATE TYPE SOLAR COLLECTORS WITH DIFFERENT DUCT PROFILES”, which he prepared after fulfilling the requirements specified in the associated legislations, before the jury whose signatures are below.

Thesis Advisor : **Prof. Dr. Figen KADIRGAN**
İstanbul Technical University

Jury Members : **Prof. Dr. Üner ÇOLAK**
İstanbul Technical University

Prof. Dr. Cem PARMAKSIZOĞLU
İstanbul Technical University

Date of Submission : **27 November 2015**
Date of Defense : **22 December 2015**

FOREWORD

I am grateful to Prof. Dr. FigenKadırgan for her valuable guidance, continuous support and positive attitude during the preparation phase of this thesis.

I would like to thank my family and friends for their motivation.

Special thanks to Istanbul Technical University for providing the licensed ANSYS software.

December 2015

Cem ÇORAPÇIOĞLU
(Mechanical Engineer)

TABLE OF CONTENTS

	<u>Page</u>
FOREWORD	vii
TABLE OF CONTENTS	ix
ABBREVIATIONS	xi
LIST OF SYMBOLS	xiii
LIST OF TABLES	xv
LIST OF FIGURES	xvii
SUMMARY	xix
ÖZET	xxi
1. INTRODUCTION	1
1.1 General	1
1.2 Purpose of the Thesis	5
1.3 Literature Review	6
1.4 Thesis Organization.....	12
2. THEORY	15
2.1 Heat Transfer Mechanism of Flat Plate Solar Air Collectors	15
2.2 Convection Heat Transfer and Internal Flow	18
2.3 Dimensionless Quantities Used in Analysis.....	21
2.3.1 Reynolds number (Re)	21
2.3.2 Nusselt number (Nu).....	22
2.3.3 Darcy friction factor (f).....	22
2.3.4 Prandtl number	23
3. NUMERICAL ANALYSIS	25
3.1 Computational Fluid Dynamics	25
3.2 Geometry	26
3.3 Meshing of the Geometry.....	30
3.4 Setup of the Simulation	30
3.4.1 . Models.....	31
3.4.2 . Materials.....	31
3.4.3 . Boundary conditions	31
3.4.4 . Solution methods.....	32
3.4.5 . Convergence criteria	32
4. NUMERICAL ANALYSIS RESULTS	33
4.1 Results and Validation	33
4.2 CFD Results for Flat Duct.....	34
4.2.1 Mesh optimization.....	34
4.2.2 Validation of turbulence model.....	35
4.2.3 Average Nusselt number	36
4.2.4 Pressure loss	37
4.2.5 Average Darcy friction factor	38
4.3 CFD Results for Finned Duct.....	38

4.3.1 Mesh Optimization.....	38
4.3.2 Average Nusselt number	39
4.3.3 Pressure loss	40
4.3.4 Average Darcy friction factor	41
4.4 Comparison of Flat and Finned Duct Types.....	42
4.4.1 Comparison of mean temperatures.....	42
4.4.2 Comparison of average Nusselt numbers.....	46
4.4.3 Comparison of pressure losses	46
4.4.4 Comparison of average Darcy friction factors	47
4.5 Thermo - Hydraulic Performance of Finned Ducts	48
5. CONCLUSIONS AND RECOMMENDATIONS	49
REFERENCES	53
CURRICULUM VITAE	57

ABBREVIATIONS

2D	: Two Dimensional
3D	: Three Dimensional
ASHRAE	: American Society of Heating, Refrigerating, and Air-Conditioning Engineers
CFD	: Computational Fluid Dynamics
HVAC	: Heating, Venting, Air Conditioning
SAH	: Solar Air Heater

LIST OF SYMBOLS

a	:Height of duct (mm)
A	:Cross sectional area (m ²)
A_c	:Surface area of absorber plate (m ²)
b	:Width of duct (mm)
c_p	:Specific heat (Jkg ⁻¹ K ⁻¹)
D_h	: Hydraulic diameter of duct (m)
f	:Darcy friction factor
h	: Local convection heat transfer coefficient (Wm ⁻² K ⁻¹)
h_{1,2,3,4}	: Forced convection heat transfer coefficients (Wm ⁻² K ⁻¹)
h_{nc}	: Natural convection heat transfer coefficient (Wm ⁻² K ⁻¹)
h_{r21,r23}	: Radiation heat transfer coefficients (Wm ⁻² K ⁻¹)
I	: Turbulent Intensity
k	: Thermal conductivity (Wm ⁻¹ K ⁻¹)
\dot{m}	: Mass flow rate (kg/s)
Nu	: Nusselt number
P	: Wetted perimeter of cross section (m)
Pr	: Prandtl number
q_s''	:Convective heat flux(Wm ⁻² K ⁻¹)
Q₂	:Heat transferred to air stream (Wm ⁻²)
Q_u	:Useful heat gain (W)
Re	: Reynolds number
S_{1,2}	: Solar radiation absorbed by surfaces(Wm ⁻²)
T	: Temperature (K)
T_{1,2,3,s}	: Surface temperatures (K)
T_a	: Ambient temperature (K)
T_{am,f,m}	: Mean fluid temperatures (K)
T_i	: Fluid inlet temperatures (K)
T_o	: Fluid outlet temperatures (K)
T_{pm}	: Mean plate temperatures (K)
T_∞	: Free stream temperature (K)
U_b	: Bottom heat loss coefficient (Wm ⁻² K ⁻¹)
U_t	: Top heat loss coefficient (Wm ⁻² K ⁻¹)
V	: Velocity (ms ⁻¹)
α	: Thermal diffusivity (m ² s ⁻¹)
ρ	: Density (kgm ⁻³)
μ	: Dynamic viscosity (kgm ⁻¹ s ⁻¹)
ν	: Kinematic viscosity (m ² s ⁻¹)

LIST OF TABLES

	<u>Page</u>
Table1.1 : Types of solar collectors	2
Table3.1 : Thermo-physical properties of working fluid (air) and absorber plate (aluminum) for computational analysis.....	31
Table4.1 :Some input and output values of numerical analysis.....	34
Table4.2 :Overall enhancement ratios for each Reynolds number.	48

LIST OF FIGURES

	<u>Page</u>
Figure1.1 : A typical flat plate solar air collector illustration.....	3
Figure 1.2 :Nonporous absorber type flat plate air collector	4
Figure1.3 :Porous absorber type flat plate air collector	4
Figure1.4 :Cross section view of new proposed duct.	5
Figure2.1 :Cross section view showing heat transfer interactions.....	15
Figure2.2 :Thermal network of a conventional type solar air collector.....	16
Figure2.3 :Three mechanisms of heat transfer.....	18
Figure2.4 :Convection heat transfer for external flow.....	18
Figure2.5 :Internal flow hydrodynamic entrance and fully developed regions	20
Figure2.6 :Internal flow thermal entrance and fully developed regions	21
Figure2.7 :Moody diagram	23
Figure3.1 :Isometric view sketch of the analyzed duct.....	27
Figure3.2 :Top view of the analyzed duct.....	28
Figure3.3 :Cross section view of conventional flat duct.....	29
Figure3.4 :Cross section view of test region for conventional duct (on top) and proposed finned duct (on bottom).....	29
Figure3.5 :Detail view showing fins of proposed duct	29
Figure3.6 :Meshing of finned duct.....	30
Figure4.1 :Change of average Nusselt number observed with different meshes.....	35
Figure4.2 :Change of average Darcy friction factors observed with different meshes.....	35
Figure4.3 :Comparison of analysis results and literature results	36
Figure4.4 :Average Nusselt number vs. Reynolds number	37
Figure4.5 :Pressure loss through duct vs. flow velocity.	37
Figure4.6 :Average Darcy friction factor vs. Reynolds number.....	38
Figure4.7 :Change of average Nusselt number observed with different meshes.....	39
Figure4.8 :Change of average Darcy friction factors observed with different meshes	39
Figure4.9 :Average Nusselt number vs. Reynolds number	40
Figure4.10 :Pressure loss through duct vs. flow velocity.	41
Figure4.11 :Average Darcy friction factor vs. Reynolds number.....	41
Figure4.12 :Temperature difference between inlet and outlet.	42
Figure4.13 :Mean plate and mean air temperature comparison of two ducts.	43
Figure4.15 :Cross section view of flat duct outlet when $Re=3000$	44
Figure4.16 :Cross section view of finned duct outlet when $Re=3000$	44
Figure4.17 :Isometric view of entry section and absorber plate of flat duct when $Re=3000$	45
Figure4.18 :Isometric view of entry section and absorber plate of finned duct when $Re=3000$	45

Figure4.19 :Average Nusselt number comparison of two ducts	46
Figure4.20 :Pressure loss comparison of two ducts.....	47
Figure4.21 :Average Darcy friction factor comparison of two ducts	47

CFD BASED THERMAL AND HYDRAULIC PERFORMANCE INVESTIGATION OF AIR HEATING PLATE TYPE SOLAR COLLECTORS WITH DIFFERENT DUCT PROFILES

SUMMARY

In this study, two different designs of solar air collector ducts were analyzed using Computational Fluid Dynamics (CFD). A conventional rectangular duct of 800mm width and 20mm height with flat absorber plate and a proposed duct with fins installed below flat absorber plate were compared within the frame of thermal and hydrodynamic properties. Fins had 1mm thickness, were 50mm apart from each other and were compressed between absorber and back plates. Modeling and steady state analysis were carried out using ANSYS Fluent 15.0 software. Two ducts were modeled in three dimensions with a depth of 2360mm, where 760mm was entrance region and 1600mm was absorber plate. Working fluid was air, duct and fin materials were aluminum. The effect of fins on air and absorber plate mean temperatures, heat distribution, heat transfer coefficient, Nusselt number, pressure drop, friction factor and performance enhancement ratio was investigated for different flow rates (from Reynolds number 3000 to 10000) and solar radiation (constant heat flux) of 1000 W/m². Standard k- ω turbulence model was employed for the analyses after confirming its accuracy by comparing analysis results with Petukhov correlation results and observing good agreement. As one of the results of the study, it was found that increase in the Reynolds number increases the thermal performance of the ducts by increasing heat transfer coefficient; and increases pressure drop. When finned duct was compared with flat duct, higher air mean temperature, lower absorber plate temperature, therefore better heat distribution; however more pressure drop was observed. Thermo hydraulic performance of finned duct was determined by calculating overall enhancement ratio in order to discuss the overall effect fins. Enhancement was not observed. Although average heat transfer coefficient was increased with the addition of fins, reduction of flow hydraulic diameter due to fins caused reduction in Nusselt number. The proposed finned duct may be feasible in real life due to its ease of construction.

FARKLI KANAL KESİTLERİNE SAHİP HAVA ISITICI GÜNEŞ KOLEKTÖRLERİNİN CFD YÖNTEMİ İLE ISIL VE HİDROLİK PERFORMANSLARININ İNCELENMESİ

ÖZET

Güneş kolektörleri güneş enerjisini içinden geçen akışkana aktaran yaygın bir yenilenebilir enerji uygulamasıdır. Bu kolektörler genellikle hava ve su ısıtmada kullanılır. Bu çalışma hava ısıtıcı güneş kolektörleri üzerinedir. Hava ısıtıcı güneş kolektörlerinde verimliliği arttırmanın önemli yöntemlerinden biri hava akışı ile ısıtıcı yüzey arasındaki ısı transferini minimum basınç kaybına yol açarak iyileştirmektir. Bu çalışmanın amacı, bir hava ısıtıcı güneş kolektörünü daha verimli hale getirebilmek için, geleneksel düz plaka soğurucu yüzeyli kolektörün akış kanalında değişiklik yaparak yeni bir alternatif önermek ve bu alternatifin performansını geleneksel kolektörün performansı ile karşılaştırmaktır. Bu doğrultuda, çalışmada düz plakalı soğurucu yüzeyli hava ısıtıcı güneş kolektörleri için, biri geleneksel diğeri önerilen olmak üzere iki farklı akış kanalı CFD (Hesaplamalı Akışkanlar Dinamiği) yöntemi ile incelenmiştir. Kanalların ısı ve hidrolik performansları incelenmiştir.

İncelenen kolektörlerin akış kanalları 20mm yüksekliğinde ve 800mm genişliğindedir. Kanallar 2360mm derinliğindedir. 1600mm soğurucu yüzey, 760mm ise ASHRAE 93-2010 standardına göre belirlenmiş giriş bölgesidir. Geleneksel düz tasarımda soğurucu yüzey sadece 800mmx1600mm boyutlarında bir plakadan oluşmaktadır. Önerilen kanal tasarımında ise soğurucu yüzey ile akış kanalının alt plakası arasına sıkıştırılmış, 1600mm boyunca devam eden, 50mm aralıklarla yerleştirilmiş 1mm kalınlığında kanatçıklar ön görülmüştür. Bu tasarımın önerilmesinde kanatçıkların iki plaka arasına sıkıştırılabilmesi ve bu sayede üretim maliyeti ve zamanından tasarruf edilebilecek olması etkili olmuştur. Zira literatürde çalışılan kanal kesitlerdeki genel problem, düşünülen kesitteki eklemelerin yada pürüzlülüklerin üretiminin zor veya yüksek maliyetli olmasıdır.

Düşünülen bu iki akış kanalının üç boyutlu modellenmesi ve sayısal analizlerinin yapılması ANSYS Fluent yazılımı ile gerçekleştirilmiştir. Sonlu hacim yöntemi ile, türbülanslı, zorlanmış konveksiyon ısı transferine maruz kalan tam gelişmiş akış için enerji, momentum ve kütle korunumu denklemleri çözdürülmüştür. Modelleme sırasında akışkan olarak hava, akış kanalının malzemesi olarak alüminyum seçilmiştir. Sadece akış kanalı ve hava modellenmiş, çevreyle etkileşim sebebiyle oluşabilecek ısı kayıpları ihmal edilmiştir. Analizler, 1000W/m² sabit ısı akısına maruz kalan soğurucu yüzey ve 3000 ile 10000 arasında değişen Reynolds sayılarına sahip hava akışı ile gerçekleştirilmiştir. Modelleme sırasında hava akış kanallarının hava akışı doğrultusunda simetrik olduğu göz önünde bulundurularak, kanalın yarısı yani 400mm x 20mm'lik kesiti modellenmiştir. Bu sayede analiz zamanlarında tasarrufa gidilmiştir. Analizlere başlamadan önce, analiz sonuçlarının gerçekçiliğinden emin olmak için bir takım testler gerçekleştirilmiştir. Öncelikle aynı

analiz, geometriyi farklı sayılarda hücrelere bölerek ve her ardışık analizde hücre sayısını arttırarak birkaç defa gerçekleştirilmiş, analizlerden elde edilen sonuçlar hücre sayısının artmasına rağmen %1'den fazla değişmediği zaman elde edilen geometri ve hücre sayısının uygunluğu teyit edilmiştir. Ayrıca farklı türbülans modellerine göre elde edilen sonuçlar literatür ile karşılaştırılarak, Standart k- ω türbülans modelinin uygunluğu teyit edilmiş ve geri kalan tüm analizler bu koşullar ile yapılmıştır.

Hava akış kanalını modelleyip analiz edebilmek için sınır şartları belirlenmesi gerekmektedir. Kanalin girişine hız sınır şartı tanımlanmıştır. Kanala hava girişi Reynolds sayısına göre belirlenen hızlarda ve 300K sabit sıcaklıkta gerçekleşmiştir. Kanalin çıkışına basınç sınır şartı tanımlanmıştır. Kanal çıkışında hava basıncının atmosfer basıncına eşit olduğu varsayılmıştır. Soğurucu yüzeye sabit ısı akışı tanımlanmıştır. Kanalin geri kalan yüzeyleri yalıtılmış kabul edilmiştir. Ayrıca tüm yüzeyler için kaymazlık sınır şartı tanımlanmıştır.

Yukarıda açıklanan koşullar altında analizler iki farklı kanal kesiti için gerçekleştirilmiştir. Analiz sonucunda, soğurucu yüzeyin ile havanın ortalama sıcaklıkları ve meydana gelen basınç kaybı kaydedilmiş, ayrıca ortalama ısı transfer katsayıları, ortalama Nusselt sayıları ve ortalama Darcy sürtünme faktörleri hesaplanmıştır. Bu parametrelere göre farklı akış kanalına sahip kolektörler karşılaştırılmıştır.

Her iki kanal için bazı ortak sonuçlar gözlemlenebilmektedir. Artan Reynolds sayılarında, yani daha hızlı hava akışı sayesinde gerçekleşen ısı transferi artmaktadır. Zira daha hızlı akış daha fazla türbülansa sebep olmaktadır ve bu sayede yüzey ve hava arasındaki ısı transfer katsayısı artmaktadır. Ancak bu durum kütleli debinin de artması anlamına geldiği için, çıkış sıcaklıklarında düşüş gözlemlenmiştir. Isı transfer performansı artmasına rağmen aynı miktardaki ısı daha fazla miktarda havayı ısıtmakta, bu yüzden çıkış sıcaklıkları yavaş akışa göre daha az olmaktadır. Bunun yanı sıra, akış hızı arttıkça kanaldaki basınç kaybının da arttığı gözlemlenmiştir.

İki farklı tasarımın karşılaştırılması CFD yazılımı ile yapıldığı için, analiz sonrasında görsel sonuçlar elde etmek de mümkün olmuştur. Fluent'ten elde edilen ısı dağılım görselleri göstermektedir ki, önerilen tasarıma eklenen kanatçıklar ısı dağılımını olumlu yönde etkilemiştir. Düz kanal için yüksek soğurucu yüzey sıcaklıkları ve nispeten düşük ortalama hava sıcaklıkları gözlemlenmişken, kanatçıklı tasarımda daha düşük soğurucu yüzey sıcaklıkları ve daha yüksek ortalama hava sıcaklıkları gözlemlenmiştir. Eklenen kanatçıklar ısıyı soğurucu yüzeyden alt yüzeye kadar iletebilmektedir. Bu sayede kanalın alt yüzeyine yakın geçen hava da ısınabilmektedir. Düz kanalda ise soğurucu yüzeye yakın akan havanın çok ısındığı, aşağıdan akan havanın ise az ısındığı ve sıcaklık dağılımında dengesizlik olduğu gözlemlenmiştir.

Ayrıca, kanatçıkların eklenmesi ile basınç kayıpları da artmıştır. Aynı miktarda hava akışı sağlayabilmek için kanatçıklı kanal düz kanala göre daha fazla enerji gerektirecektir. Yani daha fazla pompa gücüne ihtiyaç olacağı tespit edilmiştir.

Analiz sonucunda elde edilen ortalama Nusselt ve Darcy sürtünme faktörü değerleri incelendiğinde düz kanal için, kanatçıklı kanala göre daha yüksek Nusselt sayıları ve daha düşük sürtünme faktörleri gözlemlenmiştir. Bu değerlere göre önerilen tasarım düz tasarıma göre daha düşük ısı- hidrolik performans sergilemiştir. Literatürdeki benzer çalışmaların sonuçları incelendiğinde, soğurucu yüzeyin altına yerleştirilen ve

akıřta dađılmaya sebep olan pürüzlülüklerin sayesinde düz kanala göre daha yüksek ısı transfer katsayıları elde etmek mümkün olduđu görölmektedir. Ancak bu çalışmada önerilen kesitte akıř daha küçük kesitli kanallara yönlendiđi için ortalama ısı transfer katsayısı artmasına rağmen küçülen hidrolik çap sebebiyle daha düşük Nusselt sayıları gözlemlenmiştir.Önerilen kanal, üretim kolaylıđı açısından da tercih edilebilir bir tasarım olabilir.

1. INTRODUCTION

1.1 General

Through history, mankind has utilized various sources of energy. Among them are wood, coal, oil, natural gas, hydraulic potential, nuclear potential etc. Today, most commonly used energy sources are fossil fuels. However due to environmental concerns and limited reserves of fossil fuels, renewable energy is gaining importance.

Solar energy is a fundamental renewable energy source. Sun is a continuous fusion reactor that has 3.8×10^{20} MW power output. This energy is radiated outwards in all directions and 1.7×10^{14} kW of the radiation emitted is intercepted by the Earth [1]. Solar energy has been the origin of all forms of energy sources. Since the existence of Earth, solar energy is being transformed to other sources of energy. Without sun there would be no wood, coal or oil. Even the wind would not blow.

Other than the indirect effect of solar energy, the sun has been used directly by mankind in many ways. First of all, solar energy enabled edible food to grow, food to be dried and preserved; and this consequently resulted in flourishing of civilizations. With the development of civilizations, improvement of technology and increase in human needs, solar energy began to be used for more complex purposes. Today solar energy is being used in many applications such as water heating, HVAC systems, water desalination, industrial drying, electricity generation, transportation and many more. Solar energy applications can be divided into two categories: electrical applications and thermal applications.

This thesis is concerned with an important item used in thermal applications: Solar collectors. Solar collectors are special kind of heat exchanger that transform solar radiation energy to internal energy of the transport medium. The operation is simple, solar radiation is absorbed by a collector surface. It is converted to heat and transferred to transport fluid (usually air, water or oil) by means of conduction and

convection. Afterwards, the heated fluid can be used for various thermal applications.

Solar collectors have many types and they can be classified in various ways, such as air heating collectors vs. water heating collectors, flat plate collectors vs. concentrating collectors or stationary collectors vs. sun tracking collectors. Table 1.1 shows a comprehensive list of solar collectors.

Table 1.1 : Types of solar collectors [2].

Motion	Collector Type	Absorber Type	Concentration Ratio	Indicative Temperature Range (°C)
Stationary	Flat Plate Collector	Flat	1	30-80
Stationary	Evacuated Tube Collector	Flat	1	50-200
Stationary	Compound Parabolic Collector	Tubular	1-5	60-240
Single-axis Tracking	Linear Fresnel Collector	Tubular	10-40	60-250
Single-axis Tracking	Parabolic Trough Collector	Tubular	15-45	60-300
Single-axis Tracking	Cylindrical Trough Collector	Tubular	10-50	60-300
Two-axes Tracking	Parabolic Dish Reflector	Point	100-1000	100-500
Two-axes Tracking	Heliostat Field Collector	Point	100-1500	150-2000

The main goal of energy applications is to utilize the unit energy with minimum cost. Depending on the application, balance of high efficiency and low fabrication, installation, operation cost has to be established. This applies to solar collectors as well. The most efficient solar collector is not necessarily the most cost effective, therefore may not be advantageous in long run. For any type of solar collector, the designer shall consider efficient design, material costs, building costs, operation and maintenance costs all together.

In this thesis, this approach will be applied to stationary flat plate collectors that has air as the transport medium. This type of collector is the simplest type and is used for low temperature applications. A typical collector of this type can be seen in Figure 1.1. Typically, it is a box with transparent a cover sheet on top surface (glazing). Rest of the surfaces are insulated

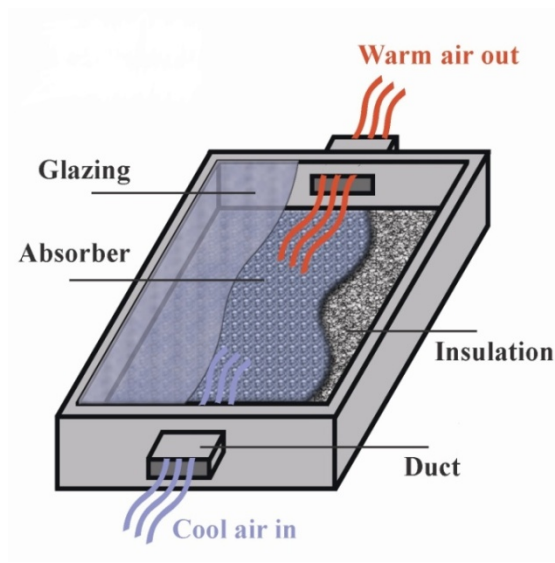


Figure 1.1 : A typical flat plate solar air collector illustration [3].

The principal element of the collector is the absorber. It is below the glazing. It enables the transfer of solar energy to transport medium as heat. There are two types of absorbers. The first type is nonporous absorber and is shown in figure 1.2. When this type is used, air stream does not flow through the absorber. Air may flow below, above or on both sides of the absorber. Nonporous absorber surface is made of materials with high thermal conductivity, usually metal sheets such as aluminum or copper. The absorber surface may be coated with special selective material in order to maximize radiant energy absorption while minimizing radiant energy emission, provided that cost effectiveness criterion is fulfilled. The second type of absorber is porous absorber and is shown in figure 1.3. When this type is used, air stream flows through the absorber. The absorber may have various designs such as slit and expanded metal, wire mesh matrix or transpired honeycomb [4].

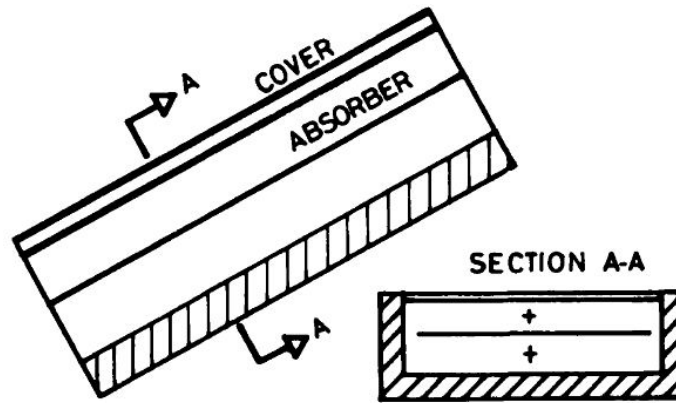


Figure 1.2 : Nonporous absorber type flat plate air collector [4].

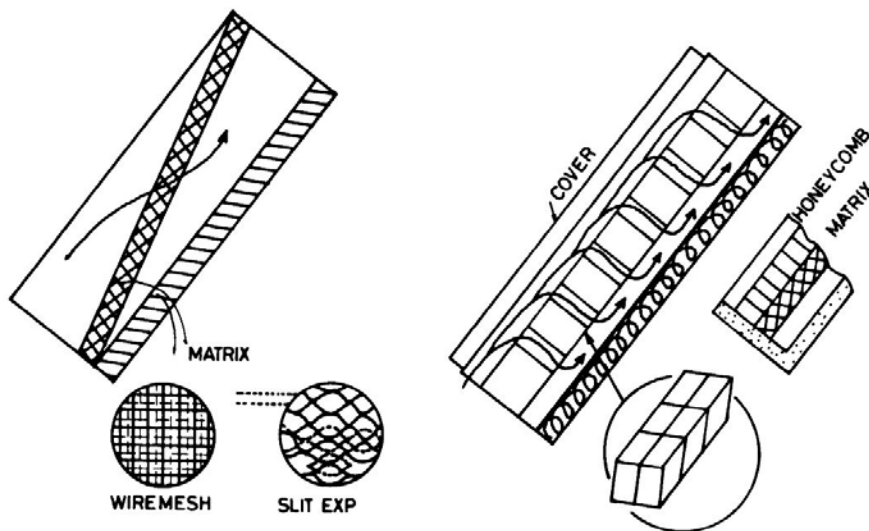


Figure 1.3 : Porous absorber type flat plate air collector [4].

Transfer of solar energy to transport medium occurs in the duct. Duct is the volume where air flowing from inlet to outlet is in contact with the absorber. While heat transfer occurs between air and absorber, all other surfaces except glazing are insulated in order to prevent heat loss.

Major issues regarding the performance of flat plate solar air heaters are due to properties of air. Reduced heat transfer properties of air results in the limitation of the heat transfer from the absorber plate to air, and causes low efficiency of heaters. Also, due to low density of air, large volumes need to be handled. Heat transfer performance improvement is possible in various methods. First of all, heaters should operate in turbulent flow regime of air to take advantage of the increased forced convective heat transfer coefficients in this regime. Turbulent flow regime can

be achieved with high flow rates. Roughening the absorber plate promotes turbulence as well and enables heat transfer enhancement, however with the cost of increased pressure drop. Improvement of performance is also possible by adding fins to absorber plate to increase heat transfer area. Other methods are to use corrugated nonporous absorber surfaces in order to improve solar flux absorption and to apply selective coating on absorber surface in order to maximize energy absorption and minimize energy emission [5].

The research in this thesis is concerned with performance improvement of flat plate solar air collectors with nonporous absorber. Considering the cons and pros of improvement methods, a new duct design is proposed. It is shown in figure 1.4. For the aim of increasing heat transfer area and turbulence, fins are placed in the duct. The usual practice is to weld the fins on absorber plate. Welding process has impact on building cost and time. To overcome these impacts, fins are compressed between absorber and back plates of the duct. When compressed with enough pressure, effect of thermal contact resistance is negligible.

The proposed duct is compared with a duct without fins by means of CFD analysis. Thermo-hydraulic properties of two ducts of same size are compared for varying flow rates and heat flux. ANSYS Fluent software is utilized to solve heat and flow equations using finite volume method.

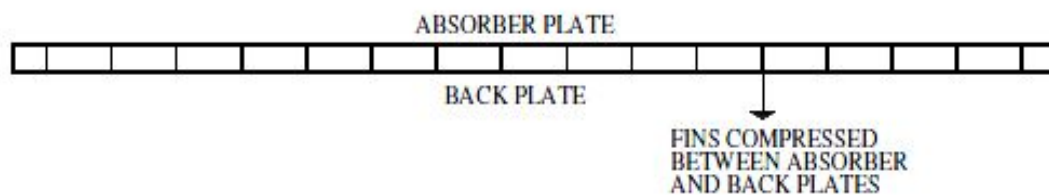


Figure 1.4 : Cross section of new proposed duct.

1.2 Purpose of the Thesis

The main objectives of this study are:

1. To comprehend factors affecting thermo-hydraulic performance of flat plate solar air collectors with nonporous absorber and to propose a new duct design for performance improvement, giving priority to ease of building.

2. To model heat transfer mechanism of the duct of flat plate solar air collectors with nonporous absorber using ANSYS Fluent CFD (Computational Fluid Dynamics) software.
3. To utilize ANSYS Fluent software to solve heat and flow equations of the system using finite volume method.
4. To compare the thermo-hydraulic performance of a flat duct and proposed new duct using the results obtained from ANSYS Fluent software simulation.

1.3 Literature Review

One of the earliest investigations on solar air heaters was made by Close. In this work, a design study was made for three basic construction types of solar air heaters. Heat transfer coefficients between the absorber plate and air stream, absorber surface material and natural convection barriers between absorber plate and ambient air varied between these three designs. It is concluded that according to calculations, these heaters can be built to provide air at 38°C above ambient, at collector efficiencies of 50 percent or more [6].

Whillier showed that the resistance to heat transfer between the air being heated and the absorbing plate has major influence on solar air heater performance, and that the efficiency of solar air heaters can be significantly improved by use of fins. Kuzay *et al.* also showed this with experimental results by comparing smooth duct with straight staggered fins and U-shaped staggered fins, obtaining higher Nusselt numbers and friction factors for both cases [7-8].

Malik and Buelow experimentally studied the hydrodynamic and thermal performances of solar air heaters with two different absorber shapes, one being a flat sheet, the other being a corrugated sheet of galvanized steel, when operated between Reynolds numbers of 10000 and 50000. Experimental results were in good agreement with theory. Major findings of this study were, duct with corrugated absorber shows better heat transfer performance, however causing more pressure drop; and improvement in heat transfer rates is lower than the rate of increase of pressure drop [9].

A study was carried out by Hollands and Shewen for optimization of air heating plate type solar collectors' flow passage geometry. In this study, they compared flat and 60

degrees V-corrugated absorber plate geometries for flows of same pressure drop and flow rate. Besides obtaining plots that show necessary parallel plate distance to give a specified pressure drop as a function of duct length and mass flow rate for flat plate collectors; they concluded that V-corrugated absorber plate has improved heat transfer performance over the flat absorber plate, collectors with duct lengths less than 1m (called short-path collectors) promise improved heat transfer performance and gain in efficiency can be obtained by increasing the emissivity of both inner and outer surfaces of flow passage [10].

In Bhargava *et al.*'s study, for three types of flat plate solar air collectors that are different from each other with the position of air flow, transient equations were solved. The effects of flow rate, absorber plate length and selective coating on collector efficiency were studied. The main conclusions were as follows: For a given flow rate, there is an optimum absorber plate length for which efficiency is maximum. For a given plate length, the efficiency increases with increasing flow rate. The selective coating will be useful only when plate length is large and flow rate is small [11].

A simple analytical model was developed by Garg *et al.* to investigate the effect of increased heat transfer area on a conventional solar air heater. Heat transfer area was increased by adding rectangular fins to flat plate absorber, or by using V-corrugated absorber plate. The design with fins was found more efficient than the design with V-corrugated absorber plate. Also, increase in efficiency was noticed with the increase in number of fins and temperature difference between inlet and outlet was found to increase with the addition of fins, the effect being more at lower flow rates [12].

Bhargava *etal.* made a comparative experimental study for two different designs of flat plate solar air heater with black painted absorber surface. Defining the efficiency of SAH as the ratio of thermal energy out and thermal energy in, double pass SAH were found to be 6-7% more efficient than single pass SAH under different weather conditions. However, effect of pressure losses on efficiency was neglected [13].

Hegazy studied on optimization of rectangular duct geometry of solar air heaters, namely finding the optimum channel depth-to-length ratio. He developed an analytical criterion that gives the minimum channel-depth required to maximize the useful heat gain from the absorber plate to the flowing air for a particular pumping

power. Later, he developed an analytical criterion that gives the optimal channel depth-to-length ratio which maximizes the collector useful energy for solar air heaters of conventional design operating at constant mass flow. Also, for variable flow operation, optimum channel depth-to-length ratio was found to be 2.5×10^{-3} . Later, he studied the applicability of this criterion to other flat plate solar air heater designs. It was concluded that the criterion is equally valid for SAH with air flow over the absorber, below the absorber, and on both sides of the absorber [14-16].

Choudhury *etal.* provided useful design curves for solar air heater designers. Curves were obtained for single pass with bare plate; single cover and double cover solar air heaters, using numerical methods. For different pressure drops and mass flow rates of air, relationship of duct length and duct depth; and relationship of heat transfer coefficient and duct length were shown. Also efficiency curves of each design were plotted as functions of air-channel length for different pressure drops and air mass flow rates; mass flow rate for fixed length of 1 m and different pressure drops; and air mass-flow rate for fixed length L of 1 m and different pumping power [17].

Metwally *et al.* experimentally investigated the performance of a solar air collector having corrugated duct. This new design was compared with five other conventional SAH designs for different air flow rates and insolation. Increased outlet air temperatures and increased efficiency was observed for new design. Efficiency could be increased even more by studying the optimum duct aspect ratio (duct depth to corrugation cycle length). Authors found the new design encouraging, as a better performance could be achieved with similar material costs [18].

Kabeel and Mecarik studied the effect of absorber shape factor on efficiency of SAH by comparing a triangular collector and a longitudinal finned collector. Being a new parameter, absorber shape factor was defined as the ratio between the total absorber area and absorber area normal to the solar radiation falling upon the collector. SAH with triangular absorber was found more efficient than the finned absorber. Also, optimum angle of the triangular absorber ranged from 50° to 60° depending on Reynolds number. The results obtained could be adapted to any solar air heater by changing the shape factor [19].

Ammar developed a mathematical model and iteratively computed the thermal performance of a single pass flat plate collector having air channels formed by slats

between the parallel plates. Performance of the proposed design was compared with the performance of conventional flat plate collector without any slats. Effects of air flow rate, collector length, spacing between the absorber and bottom plates and slat thickness were studied. Pressure losses and hydraulic performance was neglected. According to results obtained, thermal performance was enhanced with addition of slats. Increased air flow rate resulted in increased efficiency. Plate spacing of 10mm to 50mm were examined and it is observed that efficiency of the collector dropped significantly when spacing exceeds 20mm. 20mm spacing is the maximum limit. Effect of slat thickness on performance was found insignificant [20].

Karim and Hawlader experimentally compared the performance of solar air heaters having flat, V-corrugated and finned absorber surfaces. ASHRAE standard-93 test procedure was used. Each collector was designed with same inlet area. Same mass flow rate, insolation and ambient conditions were applied on all collectors; outlet temperatures were measured for various flow rates. SAH with V-corrugated absorber surface was found thermally most efficient [21].

Karim and Hawlader obtained analytical and experimental results for the thermal performance of a 60° V-corrugated plate solar air collector. Experimental results of this design indicated 12% more thermal efficiency compared to a flat plate collector. Other finding was collector efficiency's dependency on airflow rate. Efficiency increased with increasing flow rate [22].

Aharwalet *al.* made an experimental investigation on the effect of absorber surface roughness on heat transfer enhancement for a solar heater with rectangular duct. In this study, artificial roughness was applied on the absorber surface by placing repeated square cross-section split-ribs with a gap. Gap position and width varied in every design. Thermo-hydraulic performances of each duct with artificially roughened absorber were compared with that of duct with flat absorber. Increased performance was observed for the duct with roughened surface [23].

Karakaya and Durmuş manufactured and experimentally analyzed a collector that has spiral channeled ducts. With this design, route length of air flow in the duct was increased, more heat transfer and pressure drop were observed. When compared to a flat duct, new design was 31% to 45% more efficient [24].

Kumar *et al.* provided a detailed review on heat transfer enhancement of solar air heaters by using an artificial roughness technique. Results of various experimental studies that had been carried out using artificial roughness technique were presented. Developed correlations for heat transfer and friction factor were presented. Artificial roughness that is applied on absorber plate can have various geometries such as; wire, chamfered rib, v-shaped rib, transverse wedge, 90° broken transverse, transverse rib-grooved, metal grid rib roughness, transverse chamfered rib-grooved, combination of inclined and transverse ribs, dimple-shape roughness and arc shaped wire. Application of these geometries on absorber plate can vary depending on various properties such as; relative roughness pitch, relative roughness height, angle of attack and aspect ratio. The geometry and application factors of the roughness, as well as the Reynolds number of the air flow affect heat transfer performance and pressure drop of the absorber. Knowing these parameters, it is possible to determine correlations for friction factor and Nusselt number [25].

El-Sebaïet *et al.* theoretically and experimentally investigated the thermo-hydraulic performances of double pass finned plate solar air heater and double pass v-corrugated plate solar air heater. The results showed that the double pass v-corrugated plate solar air heater is 9.3% to 11.9% more efficient than the double pass finned plate solar air heater. Also, for both types flow rates that resulted in maximum thermos hydraulic efficiency were reported. It was observed that after a peak flow rate, increase in thermal efficiency was insignificant [26].

Recently, with the improvement of computer technologies, solar collectors are being investigated using computational fluid dynamics (CFD) software. Ingle *et al.* presented CFD analysis of a flat plate solar collector. The aim was to verify theoretical and experimental work done, using CFD tool. Due to some limitations of experimental and theoretical results, it was not possible to get data for each and every point on the collector. By utilizing CFD tool, it was possible to understand the flow and temperature distribution of air through solar flat plate collector. A similar study was carried out by Chaudhari *et al.* for a collector having wavy structured absorber plate. Results of CFD study were verified with experimental data and CFD study was considered reliable [27-28].

Amraoui and Aliane performed a CFD simulation of flat plate solar air collector. The collector had been experimentally analyzed before. To verify CFD results, outlet

temperature of air was compared with experimental results and good agreement was observed. The simulated collector's duct had longitudinal baffles that did not touch the absorber, but had the role of extending the flow and reducing the effect of dead zones. Because of the baffles, contact between the air and absorber increased and improved efficiency was achieved. With the aid of CFD tool, flow and temperature distribution inside the duct were visualized in three dimensions. Also, turbulence and velocity profiles were plotted against position in duct for duct with and without longitudinal baffles to understand effect of baffles [29].

Yadav and Bhagoria presented a detailed review of studies that dealt with the application of CFD in the design of solar air heater. Before review of the studies, description of solar air heater thermo-hydraulic performance was made. Computational approach in solving a problem of fluid flow and heat transfer is explained and elements of CFD codes were presented. After review of the studies, emphasis was given on the turbulence models used by CFD codes and a comparison study was carried out to find best turbulence model for a two dimensional flat plate duct flow. Results obtained from renormalization-group $k-\epsilon$ turbulence model showed the best agreement with Dittius-Boelter and Blasius empirical correlations [30].

Many CFD studies have been performed to observe heat transfer enhancement of solar air heaters by using an artificial roughness technique. In these studies, ducts having absorber surfaces roughened by artificial roughness was modeled in either 2D or 3D; boundary conditions and turbulence model to be used were determined; and continuity, momentum and energy equations were solved for the solution of heat transfer and flow analysis problems by the CFD code. Thermo-hydraulic performance of proposed ducts was analyzed with Nusselt number vs. Reynolds number and friction factor vs. Reynolds number values and correlations obtained from CFD simulation results. Performance enhancement was observed for all cases. A summary of such studies are below.

Chaube *et al.* carried out a 2D CFD analysis to compare performances of different roughness elements attached on the absorber plate. Roughness elements were rectangular, square, chamfered, triangular and semicircle ribs. SST $k-\omega$ turbulence model was utilized for flows ranging from Re 3000 to Re 20000. According to results, chamfered ribs were not effective because heat transfer enhancement was

small, but friction factor increase was large. Rectangular ribs gave the best thermos-hydraulic performance [31].

Kumar and Saini carried out a 3D CFD analysis for solar air heater having roughened absorber plate with artificial roughness in arc shaped geometry. Renormalization-group $k-\varepsilon$ turbulence model was used. For the same roughness geometry, different relative roughness height and relative arc angle were compared. Maximum enhancement ratio obtained was 1.7 [32].

Nayak *et al.* carried out a 2D CFD analysis to examine the heat transfer and flow characteristics of a duct having an absorber with artificial roughness in the form of square ribs. For the analysis, $k-\omega$ turbulence model was utilized, Reynolds number ranged from 3000 to 15000. Artificial roughness was analyzed for different relative roughness pitch. According to analysis, peak in local heat transfer occurs at the point of reattachment of the separated flow. Analysis is confirmed with experimental results [33].

Yadav and Bhagoria studied heat transfer and fluid flow processes in an artificially roughened solar air heater by using 2D CFD simulation. Artificial roughness was transverse wire ribs that had diameters of 0.7mm, 1mm and 1.4mm attached below absorber plate. Simulation was carried out for each wire diameter for different Reynolds number and different relative roughness pitch. Analysis was performed using the commercial ANSYS Fluent 12.1 code. Renormalization-group $k-\varepsilon$ turbulence model was used. Thermo-hydraulic enhancement factor varied from 1.1 to 1.65 for different combinations of relative roughness height, relative roughness pitch and Reynolds number. The authors (2014) made a similar study for a solar air heater duct that had equilateral triangular sectioned rib roughness on the absorber plate. Same software and turbulence model was utilized, and same parameters were observed. Thermo-hydraulic enhancement factor varied from 1.35 to 2.11 for different combinations of relative roughness height, relative roughness pitch and Reynolds number [34-35].

1.4 Thesis Organization

The thesis consists of five chapters. Chapter one is the introduction, where the subject is introduced with the review of theoretical, numerical and experimental

studies that have been carried out in order to find methods for enhancing thermo-hydraulic performance and increasing the efficiency of solar air heaters.

Chapter two presents the theory. Flat plate solar air heaters, especially the heat transfer mechanisms are explained in detail.

Chapter three introduces the ducts to be analyzed and describes how ANSYS Fluent software is utilized and how the simulation is carried out. Modeled geometries, meshing process, mathematical models used, boundary conditions given and solution methods used are presented in detail.

Chapter four presents the simulation results. Thermal and hydraulic performance of two different duct profiles are presented and compared.

Chapter five provides the conclusions and recommendations.

2. THEORY

2.1 Heat Transfer Mechanism of Flat Plate Solar Air Collectors

A flat plate collector generally consists of a transparent glass cover, an absorber plate and a parallel back plate. Depending on the type of fluid, that is air or water, the flow passage is designed. For air as working fluid, the gap between the absorber plate and back plate is made passage for the flow of fluid. The collector is insulated from the sides and the bottom to further minimize the heat loss. A glass cover at the top helps to reduce the convective and radiative heat losses from the absorber plate to the outside air.

Various other designs are also possible, such as double pass design, where air flow both above and below the absorber plate, or design with no glazing, where absorber plate is directly exposed to ambient, or design without back plate, where air flows between the glazing and absorber plate.

Figure 2.1 shows a cross section view of the most conventional type solar air collector, where heat transfer mechanism of each component can be seen. T_1 is the transparent glass cover, T_2 is the absorber plate and T_3 is the back plate [36].

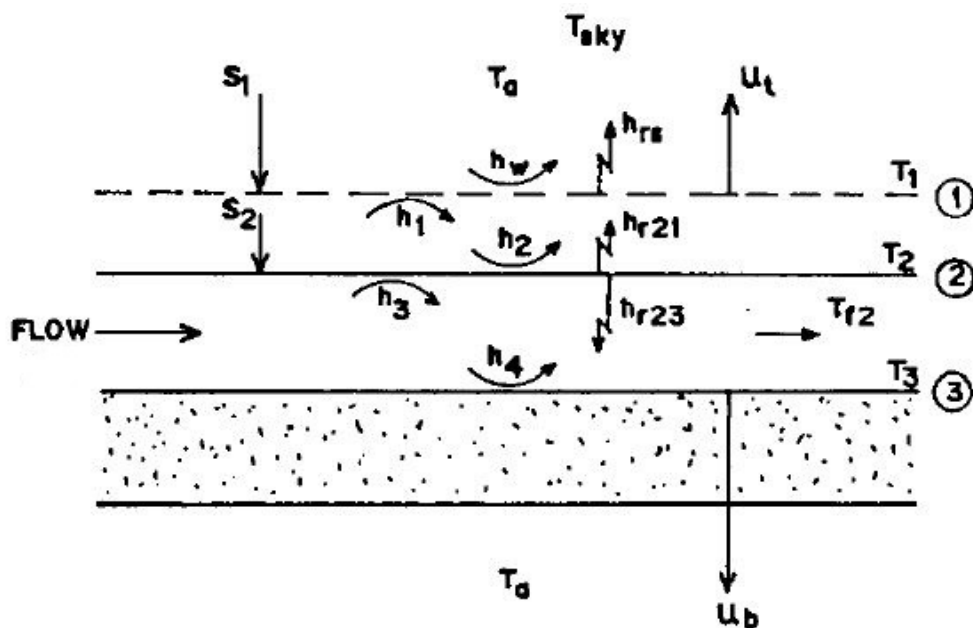


Figure 2.1 : Cross section view showing heat transfer interactions [36].

Figure 2.2 shows the thermal network in accordance with Figure 2.1. It is possible to develop heat balance equation for each point. Equations (2.1 - 2.4) are heat balance equations for T_1 , T_2 , T_{f2} and T_3 , respectively.

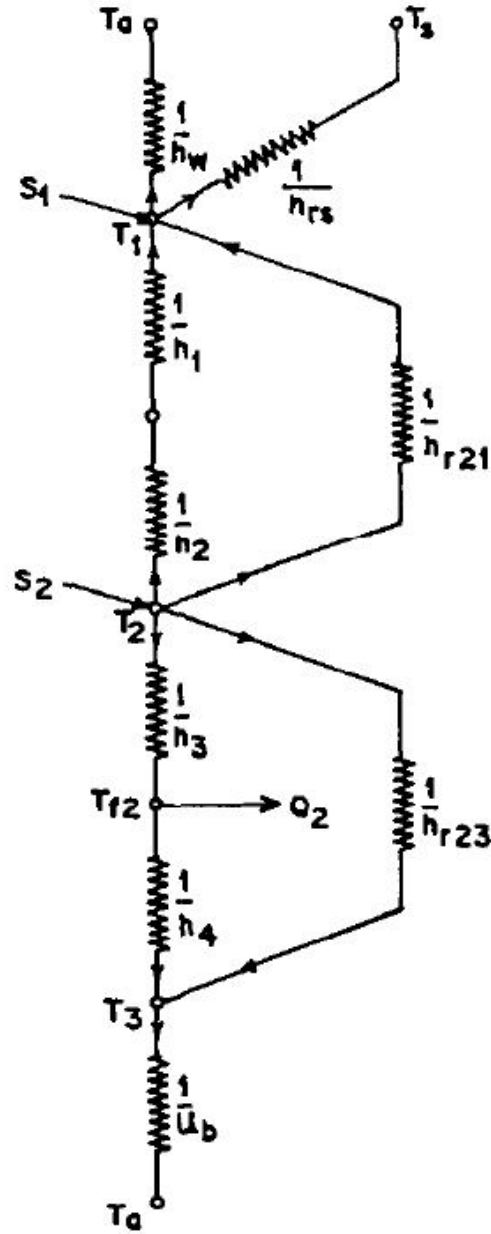


Figure 2.2 : Thermal network of a conventional type solar air collector [36].

$$S_1 + h_{r21}(T_2 - T_1) + h_{nc}(T_2 - T_1) = U_t(T_1 - T_a) \quad (2.1)$$

$$S_2 = h_3(T_2 - T_{f2}) + h_{nc}(T_2 - T_1) + h_{r23}(T_2 - T_3) + h_{r21}(T_2 - T_1) \quad (2.2)$$

$$h_3(T_2 - T_{f2}) = h_4(T_{f2} - T_3) + Q_2 \quad (2.3)$$

$$h_4(T_{f2} - T_3) + h_{r23}(T_2 - T_3) = U_b(T_3 - T_a) \quad (2.4)$$

where $h_{1,2,3,4}$ are forced convection heat transfer coefficients, h_{nc} is natural convection heat transfer coefficient, $h_{r21,r23}$ are radiation heat transfer coefficients, Q_2 is the heat transferred to air stream, $S_{1,2}$ are solar radiation absorbed by surfaces, $T_{1,2,3}$ are temperature of surfaces, T_a is ambient temperature, T_f is mean fluid temperature, U_b is bottom heat loss coefficient and U_t is top heat loss coefficient.

The thermal network and developed equations clearly show that thermal behaviors of all components depend on each other. For example Q_2 , the heat transferred to air stream depends on temperature of bounding plates and forced convection heat transfers. At the same time T_2 , the absorber plate temperature depends on S_2 , solar radiation absorbed by the surface and h_{r21} , radiation heat transfer coefficient of the surface. Such relations exist for all components and can be read from the network and equations.

Efficiency of a solar air collector depends on all of the above parameters. The studies summarized in Chapter 1 had tried different variations of collectors in order to change the affecting parameters and have better performance. For example, using a selective surface as absorber plate increases S_2 and reduces h_{r21} , therefore results in higher T_2 . Or adding roughness elements on absorber plate increases turbulence and h_3 , therefore results in higher Q_2 .

This thesis is concerned with duct flow of a collector. The rate of valueable energy gain by flowing air in the duct of a air heating solar collector can be calculated from equation (2.5). This equation is the heat transfer balance, and shows the relationship of valueable energy with air mass flow rate, specific heat of air, inlet and outlet temperatures, as well as the relationship of valuable energy with heat transfer coefficient, heat transfer area, mean absorber and air temperatures.

$$Q_u = \dot{m}c_p(T_o - T_i) = hA_c(T_{pm} - T_{am}) \quad (2.5)$$

The value of heat transfer coefficient, h , can be increased by various techniques. So the aim of such study is to find a way to increase heat transfer to air, at the same time

minimizing pressure drop. Such study is concerned with the fluid and surface interactions. So, the case is simplified to a convection heat transfer problem for internal flow. In order to proceed, good comprehension of internal flow is necessary.

2.2 Convection Heat Transfer and Internal Flow

Heat transfer is thermal energy in transit due to a spatial temperature difference. Whenever a temperature difference exists in a medium or between media, heat transfer must occur. As shown in Figure 2.3, heat transfer can occur in three ways: Conduction, convection and radiation. All three mechanisms are active for a case of solar air collector, however for the case of duct flow, only convection will be explained in detail.

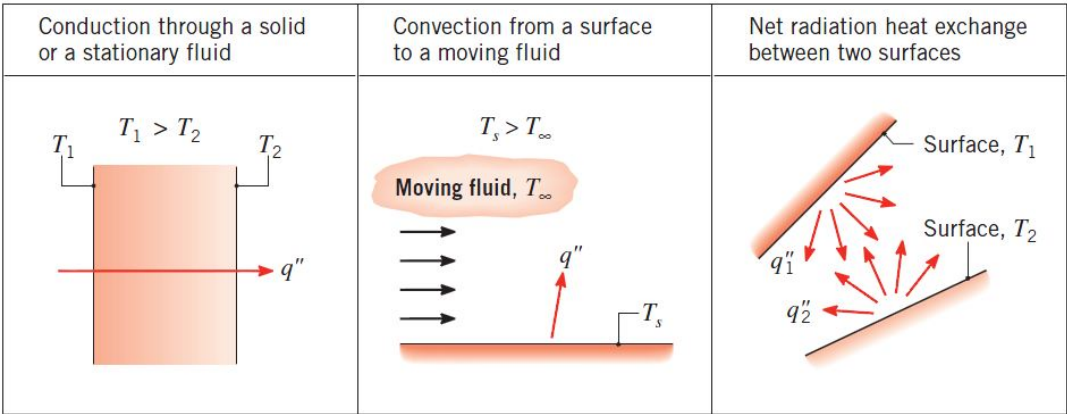


Figure 2.3 : Three mechanisms of heat transfer [37].

Convection can be described as the energy transfer between a surface and a fluid moving over the surface which are at different temperatures. Convection includes energy transfer by both the bulk fluid motion and the random motion of fluid molecules.

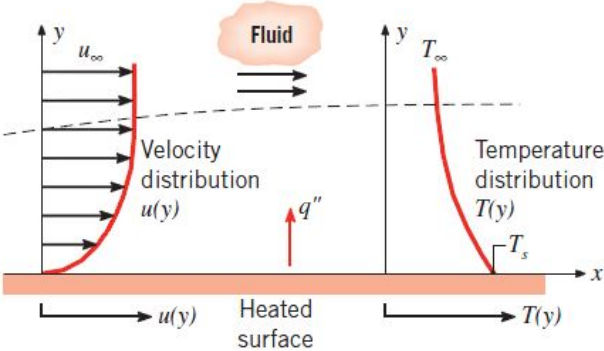


Figure 2.4 : Convection heat transfer for external flow [37].

Figure 2.4 shows fluid flow over a heated surface. As a result of the fluid–surface interaction, a region is developed in the fluid through which the velocity varies from zero at the surface to a finite value u_∞ associated with the flow. This region of the fluid is known as the hydrodynamic or velocity boundary layer. Moreover, as the surface and flow temperatures are different, there will be a region of the fluid through which the temperature varies from T_s at surface to T_∞ in the outer flow. This region is called as the thermal boundary layer. The velocity boundary layer is characterized by the presence of velocity gradients and shear stresses. The thermal boundary layer is characterized by temperature gradients and heat transfer.

The basic rate equation of convection heat transfer for internal flow is of the form equation (2.6)

$$q_s'' = h(T_s - T_m) \quad (2.6)$$

where, the convective heat flux q_s'' , is proportional to the difference between the surface and flow mean temperatures, T_s and T_m , respectively. The mean temperature is reference temperature for internal flows, playing the role as the free stream temperature T_∞ shown in Figure 2.4. However T_m varies in flow direction whereas T_∞ is constant. This equation (2.6) is known as Newton's law of cooling, and the parameter h is the local convection heat transfer coefficient. This coefficient depends on conditions in the boundary layer, which are influenced by surface geometry, the nature of the fluid motion, and an assortment of fluid thermodynamic and transport properties. Any study of convection ultimately reduces to a study of the means by which h may be determined [37].

An essential step in the treatment of any convection problem is to determine whether the boundary layer is laminar or turbulent. Surface friction and the convection transfer rate depend significantly on this condition. The main difference between laminar and turbulent flow, in the case of heat transfer, is that an additional mechanism of heat transfer in the radial and azimuthal directions becomes available in turbulent flow. This provides much better transfer of energy across the flow at a given axial position than in laminar flow, wherein conduction is typically the only mechanism that operates in the transverse directions.

Flows can be categorized as internal or external. External flow is the case where the flow is unbounded from above. Internal flow occurs when the flow is bounded, such as in a pipe or duct. This difference results in different boundary layer development characteristics. Concepts of hydrodynamic and thermal entrance and fully developed regions are introduced with internal flow.

Hydrodynamic entrance region, shown in Figure 2.5 begins by development of velocity profile near the entrance of the pipe or duct. A velocity boundary layer grows on the pipe wall and eventually merges on the center line of the pipe. At this point the flow becomes hydrodynamically fully developed. Skin friction and pressure losses are greater in the entrance region. Friction factor f becomes a constant once the velocity profile is fully developed.

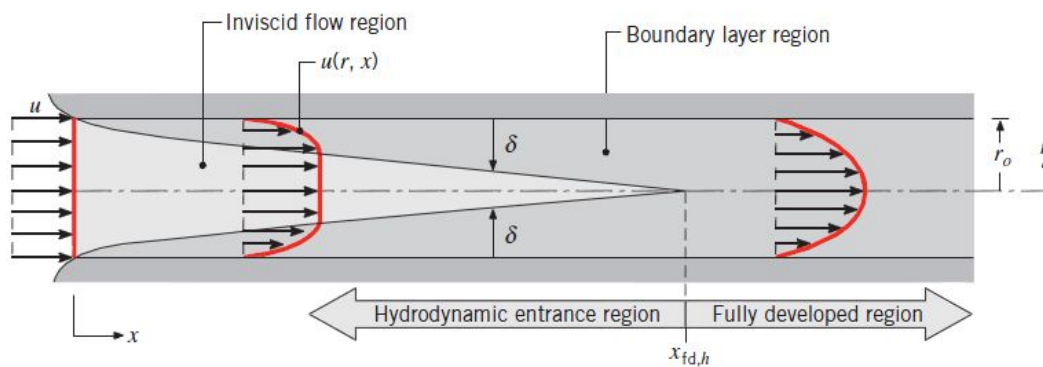


Figure 2.5 : Internal flow hydrodynamic entrance and fully developed regions [37].

Thermal entrance region, shown in Figure 2.6 begins by development of temperature profile near the entrance of the pipe or duct. A thermal boundary layer grows on the pipe wall and eventually merges on the center line of the pipe. At this point the flow becomes thermally fully developed. Convective heat transfer rate is higher in the entrance region, it becomes a constant once the flow is thermally fully developed. Thermal entrance region is relatively short in turbulent flow, whereas it tends to be long in laminar flow.

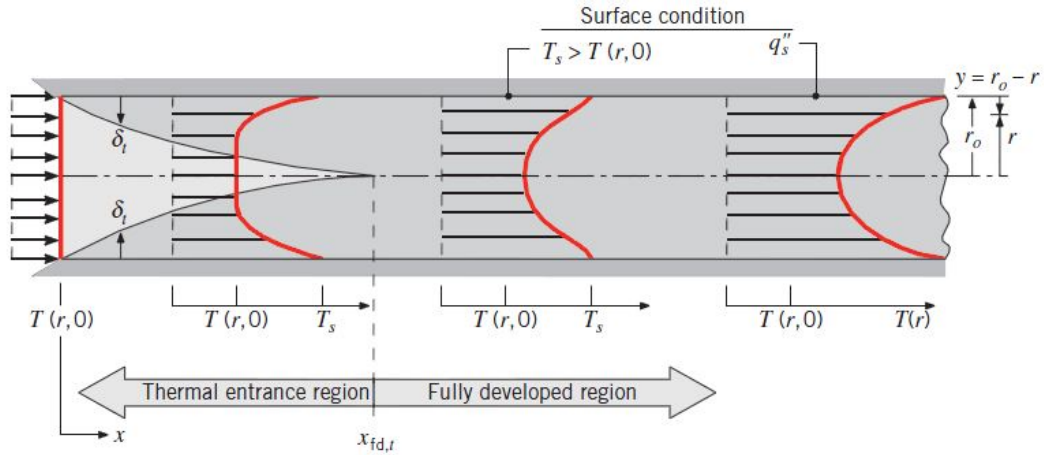


Figure 2.6 : Internal flow thermal entrance and fully developed regions [37].

2.3 Dimensionless Quantities Used in Analysis

2.3.1 Reynolds number (Re)

Reynolds number is a dimensionless quantity that is used to help predict similar flow patterns in different fluid flow situations. Reynolds number is defined as the ratio of momentum forces to viscous forces. It quantifies the relative importance of these two types of forces for given flow conditions.

Reynolds number is used to characterize if a flow is in laminar or turbulent regime. Laminar flow occurs at low Reynolds numbers and is dominated by viscous forces, and is characterized by smooth, constant fluid motion. Turbulent flow occurs at high Reynolds numbers and is dominated by inertial forces, and chaotic eddies, vortices and other flow instabilities are produced. For internal flows, according to experimental observations, laminar flow occurs when $Re < 2300$, turbulent flow occurs when $Re > 4000$. For values in between, both laminar and turbulent flows are possible and the range is called as transition region.

For internal flow, Reynolds number is defined in equation (2.7).

$$Re = \frac{\rho V D_h}{\mu} = \frac{V D_h}{\nu} \quad (2.7)$$

where ρ is density of fluid, V is velocity of fluid, D_h is hydraulic diameter of the duct, μ is dynamic viscosity of the fluid and ν is kinematic viscosity of the fluid.

D_h , hydraulic diameter is a term used in flow calculations of non-circular tubes and channels. For a circular tube, hydraulic diameter is basically the diameter of the tube. For non-circular tubes, it is defined in equation (2.8)

$$D_h = \frac{4A}{P} \quad (2.8)$$

where, A is the cross sectional area and P is the wetted perimeter of the cross section.

2.3.2 Nusselt number (Nu)

In heat transfer, Nusselt number is the ratio of convective heat transfer to conductive heat transfer across a surface. Nusselt number close to unity represents the case of slug flow, where convection and conduction are at similar magnitudes. Turbulent flows have larger Nusselt numbers. A larger Nusselt number corresponds to more active convection. Nusselt number is defined in equation (2.9).

$$Nu = \frac{hD_h}{k} \quad (2.9)$$

where, h is the convective heat transfer coefficient of the flow and k is the thermal conductivity of the fluid.

2.3.3 Darcy friction factor (f)

Darcy friction factor is a dimensionless quantity used for the description of friction losses in flows. It is the resistance coefficient parameter in Darcy-Weisbach equation, which relates pressure loss, due to friction along a given length of pipe to the average velocity of the fluid flow for an incompressible fluid. Darcy friction factor can be obtained from Moody diagram. Shown in Figure 2.7, Moody diagram is a family of curves that relate friction factor, Reynolds number and relative roughness of a pipe.

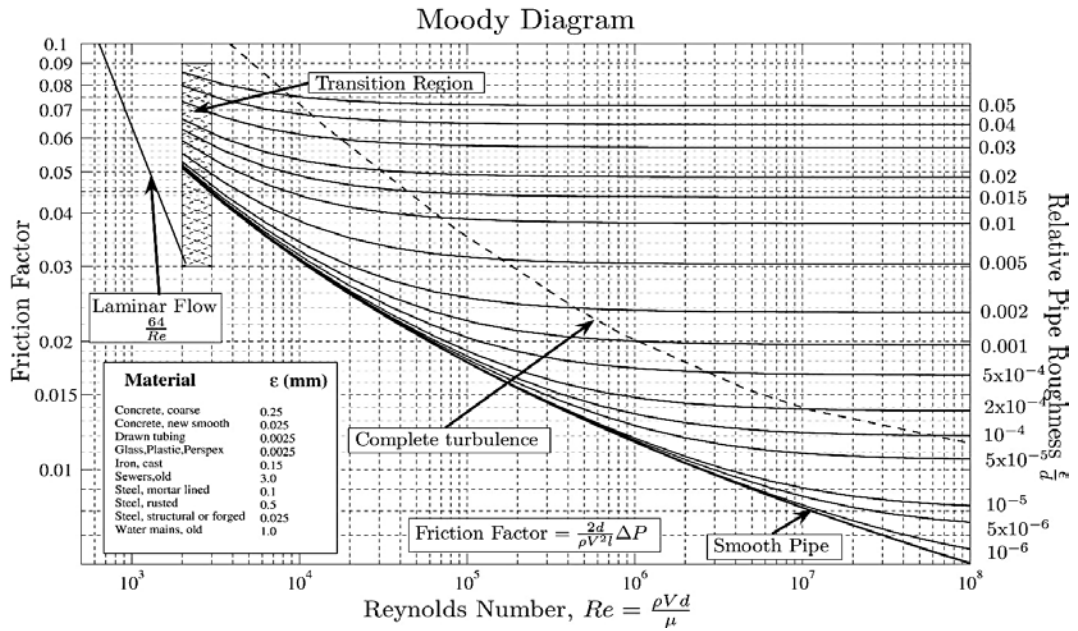


Figure 2.7 : Moody diagram [38].

2.3.4 Prandtl number

Prandtl number is the ratio of momentum diffusivity to thermal diffusivity. In heat transfer cases, Prandtl number controls the thickness of hydrodynamic and thermal boundary layer thicknesses. For $Pr = 1$, two boundary layers have the same thickness. For $Pr < 1$, hydrodynamic boundary layer is thinner than thermal boundary layer, meaning that heat diffuses quicker than momentum. For $Pr > 1$, hydrodynamic boundary layer is thicker than thermal boundary layer. Prandtl number ranges between 0.7 and 0.8 for air and many other gases. It is defined in equation (2.10).

$$Pr = \frac{\nu}{\alpha} = \frac{c_p \mu}{k} \quad (2.10)$$

where ν is momentum diffusivity or kinematic viscosity, α is thermal diffusivity, c_p is specific heat, μ is dynamic viscosity and k is thermal conductivity.

3. NUMERICAL ANALYSIS

A technical problem, such as the subject of this thesis, can be solved with analytical, experimental or numerical methods. Although reliable solution can be obtained using experimental method, this method may be costly and time consuming due to required apparatus or other factors. On the other hand, analytical methods are functional for linear problems. Non-linear problems, such as turbulent flow can be linearized and solved using numerical methods. In this study, numerical methods are used for the case of turbulent flow and heat transfer in a solar collector duct. For this purpose, ANSYS Computational Fluid Dynamics simulation software is used. ANSYS Fluent Release 15.0 CFD tool is utilized.

3.1 Computational Fluid Dynamics

Computational Fluid Dynamics (CFD) is the science of predicting fluid flow, heat and mass transfer, chemical reactions, and related phenomena by solving numerically the set of governing mathematical equations that are, conservation of mass, conservation of momentum, conservation of energy, conservation of species, effects of body forces [39].

ANSYS CFD solvers are based on the finite volume method. Domain is discretized into a finite set of control volumes. After the solution domain is divided into very large number of sub-zones, general conservation (transport) equations (3.1) for mass, momentum, energy, species, etc. are solved on this set of control volumes according to given boundary conditions. Partial differential equations are discretized into a system of algebraic equations. All algebraic equations are then solved numerically to render the solution field. During the solution process, any small change occurring in the properties of the fluid at a point is used in the input to next node point. This procedure is repeated for all grid points; the end result of this computation is that all the properties, like temperature, velocities etc at all the points in the domain are eventually known. At the end, results can also be obtained in visual form [39].

$$\frac{\delta}{\delta t} \int_V \rho \phi dV + \oint_A \rho \phi V \cdot dA = \oint_A \Gamma \nabla \phi \cdot dA + \int_V S_\phi dV \quad (3.1)$$

When $\Phi = 1$, continuity equation is obtained; when $\Phi = u$, X momentum equation is obtained; when $\Phi = v$, Y momentum equation is obtained; when $\Phi = w$, Z momentum equation is obtained; when $\Phi = h$, energy equation is obtained.

CFD modeling was originally developed for industrial application. Today it is used in research work, product development, and in almost any case where a detailed understanding of phenomena involving heat transfer, fluid flow or phase change is desired. A number of software based on CFD codes have been developed, few of them are: Fluent, Flovent, Phoenics, and CFX. Each software is usually supported by supplementary software for different applications, such as domain model preparation, mesh generation etc. Recently CFD tools are increasingly used to model flow through solar collectors [40].

3.2 Geometry

Duct of a solar air collector was modelled in this thesis. Two different designs of solar air collector ducts were considered. A common isometric sketch of ducts is shown in Figure 3.1. For both of them, the flow system consists of 760 mm long entry section and 1600 mm long test section, shown in Figure 3.2. The entry length of the flow has been kept to achieve fully developed flow at the test section and to reduce the end effects on the test section considering the recommendation provided in ASHRAE Standard 93-2010 [41].

$$LengthofEntranceRegion = 6\sqrt{a * b} \quad (3.2)$$

where a is the height and b is the width of the air collector air flow opening.

Figure 3.3 and Figure 3.4 show different cross sections of the ducts. They have cross sectional dimensions of 800 mm x 20 mm. Figure 3.3 shows the duct of a conventional flat plate collector. There is no insertion in the duct, so the air flows through a smooth rectangular duct. Figure 3.4 shows the difference between two ducts. For the proposed duct, fins of 1mm thickness are installed with 50mm distance between them. Figure 3.5 shows the fin detail. At cross section B-B, for both

ductsides and bottom face are insulated and top face is the absorber, only surface where heat flux is applied. For the proposed duct, fins are only present in test region, between the absorber plate and back plate.

Modeling is done in 3D using ANSYS Design Modeler software. Since both of the duct geometries are symmetric with respect to axis of flow direction, only half of the duct was modeled to save computational power and time. In the modeled case, cross sectional dimensions are 400 mm x 20 mm and the cut face is defined as symmetry boundary condition.

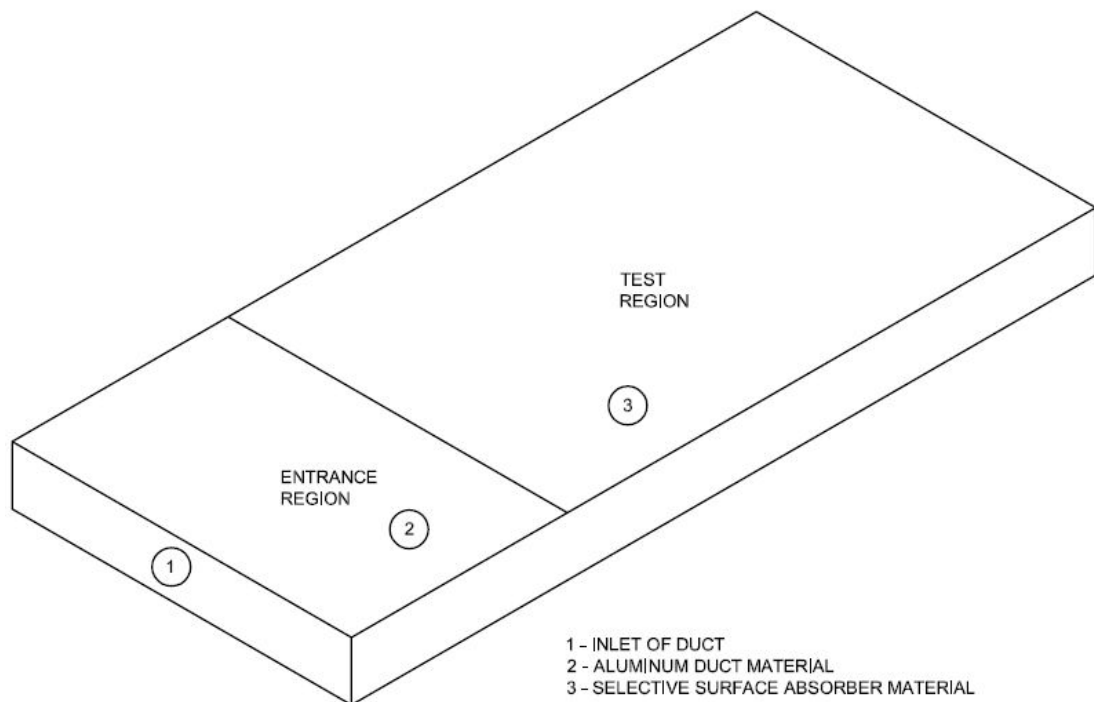


Figure 3.1 : Isometric view sketch of the analyzed duct.

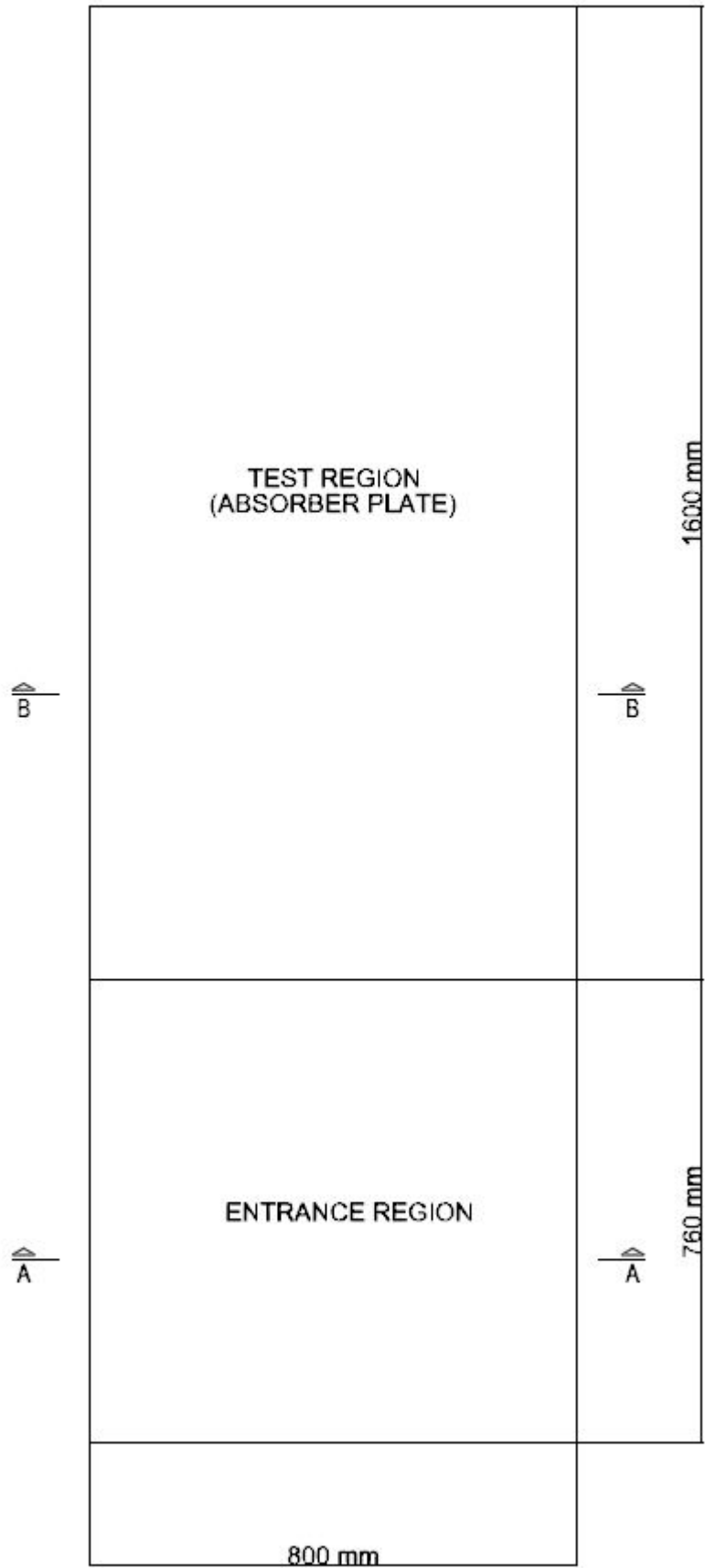


Figure 3.2 : Top view of the analyzed duct.

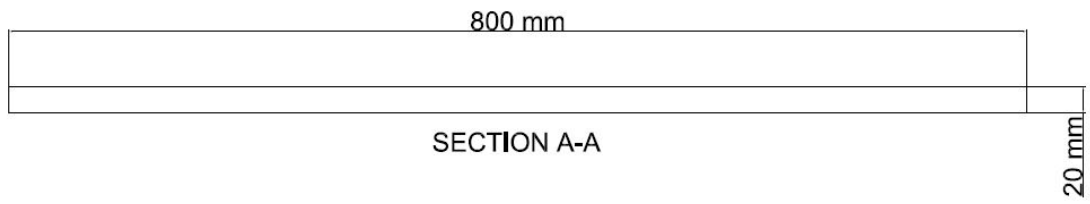


Figure 3.3 : Cross section view of conventional flat duct.

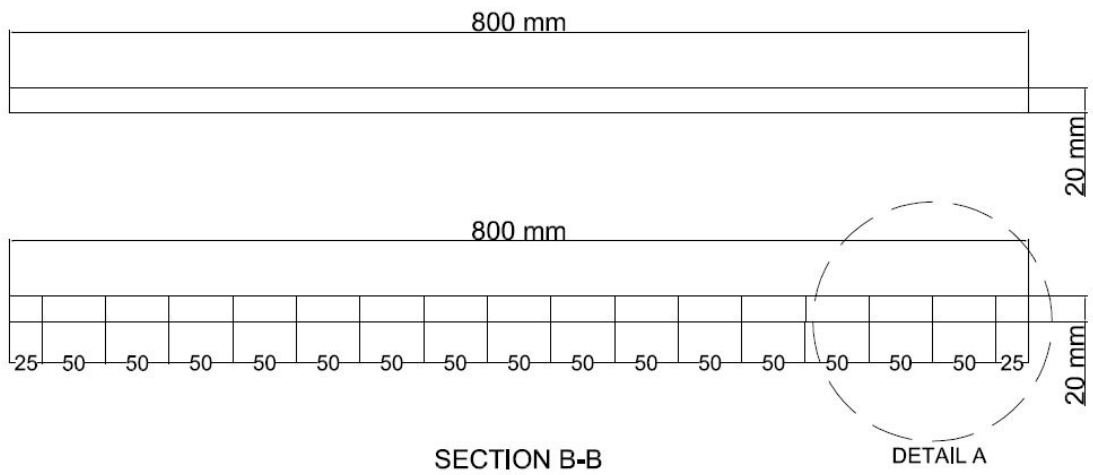


Figure 3.4 : Cross section view of test region for conventional duct (on top) and proposed finned duct (on bottom).

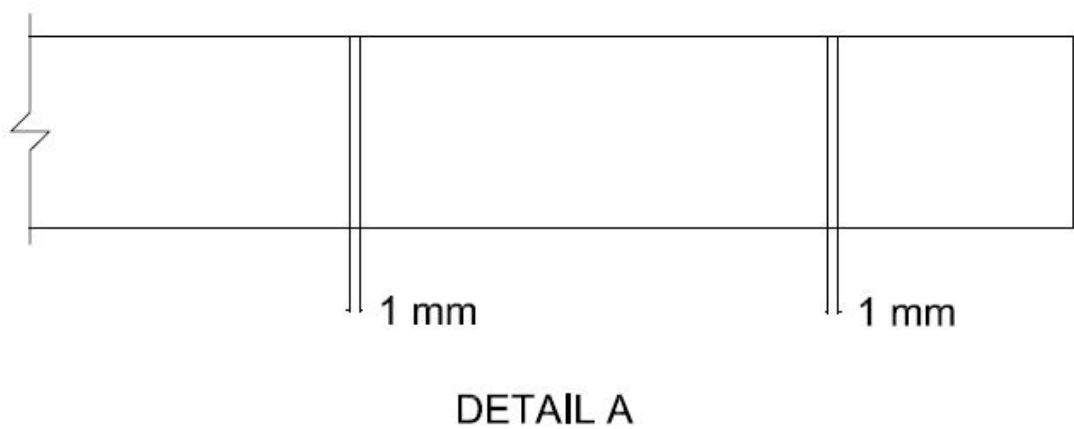


Figure 3.5 : Detail view showing fins of proposed duct

3.3 Meshing of the Geometry

Fluent Meshing software was used. In order to examine the flow and heat transfer critically close to heat transfer regions, finer meshing at these locations has been done. In other regions coarser mesh has been used. This can be seen in Figure 3.4.

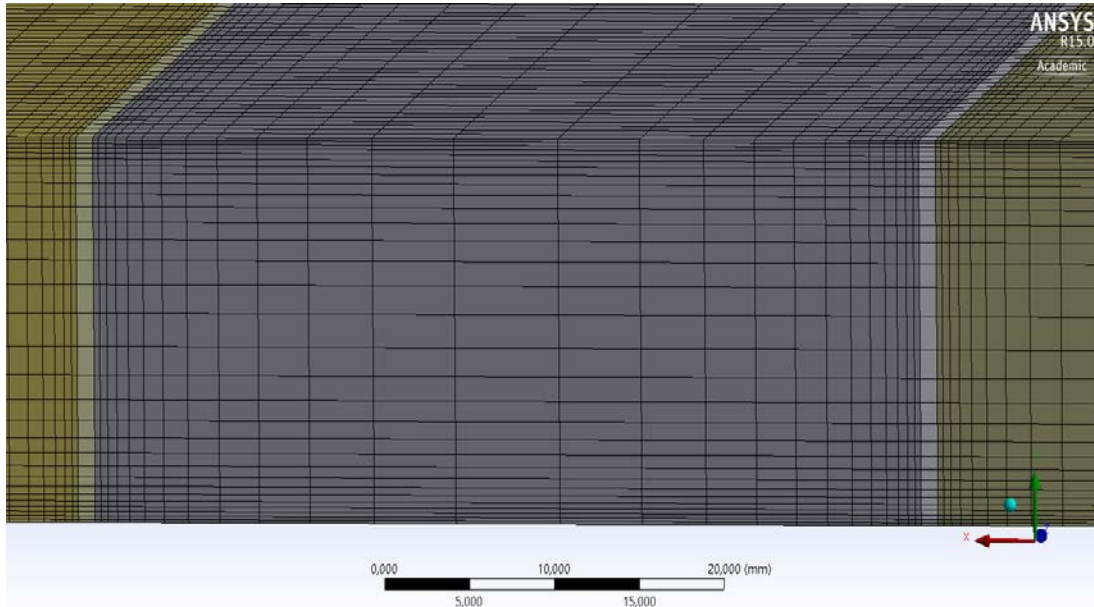


Figure 3.6 : Meshing of finned duct.

Due to the simplicity and cleanness of the duct geometries, hexagonal elements could be used for meshing. Elements are aligned in direction of air flow. Sweep meshing method is used.

3.4 Setup of the Simulation

ANSYS Fluent software was used to define the mathematical model for the geometry and grids created in previous steps. Double precision option was chosen. Pressure-based and steady state solver was utilized. Then, models were chosen, boundary conditions and materials were defined, solver settings and convergence criteria were chosen, calculation was initialized and the model was ready for calculation.

The following assumptions were made for this simulation:

- i. The flow is turbulent, three dimensional and fully developed in test region.
- ii. The thermal conductivity of the duct wall and fins does not change with temperature.
- iii. The duct wall and fin material is homogeneous and isotropic.

- iv. The working fluid is assumed to be incompressible for operating range of solar air heaters since variation in density is very less.
- v. Negligible radiation heat transfer and other heat losses.

3.4.1 . Models

To solve for heat transfer, energy equation was enabled. For the modeling of turbulence terms in conservation equations, Standard k- ω turbulence model was chosen. This model is suitable for turbulent flows with Reynolds number 10000 and smaller. Validity of this turbulent model was confirmed by comparing the simulation results with correlations applied in literature.

3.4.2 . Materials

Materials chosen are, air for fluid flow and aluminum for all parts of the duct, including absorber plate and fins. Table 3.1 shows the material properties.

Table 3.1 : Thermo-physical properties of working fluid (air) and absorber plate (aluminum) for computational analysis.

Properties	Unit	Working fluid (air)	Absorber plate (aluminum)
Density - ρ	kg m ⁻³	1.225	2719
Specific heat - C_p	J kg ⁻¹ K ⁻¹	1006.43	871
Viscosity - μ	N s m ⁻²	1.79E-05	-
Thermal conductivity - k	W m ⁻¹ K ⁻¹	0.0242	202.4
Prandtl Number		0.7441	-

3.4.3 . Boundary conditions

The boundaries of a duct are inlet, outlet and the surrounding walls. As stated in part 3.2, one of the side walls was defined as symmetry boundary condition. Rest of the surrounding walls are in contact with the fluid and no-slip boundary condition was assigned on them, meaning that the velocities of air on the wall surface are zero. All walls are adiabatic, except absorber surface. 1000 W/m² constant heat flux thermal boundary condition was defined on the absorber plate.

Velocity boundary condition was defined for the inlet of the duct. Velocity, turbulent intensity and hydraulic diameter was necessary to define boundary condition. The mean inlet velocity of the flow was calculated using Reynolds number. Turbulent

intensity was calculated according to (3.3). Hydraulic diameter was calculated according to (3.4). Inlet temperature of air was taken 300 K.

$$I = 0,16(Re)^{-1/8} \quad (3.3)$$

$$D_h = \frac{4 * (Area)}{(Perimeter)} \quad (3.4)$$

Pressure boundary condition was defined for the outlet of the duct. Pressure, turbulent intensity and hydraulic diameter was necessary to define boundary condition. Pressure was taken 0 Pa. It was assumed that the fluid reaches atmospheric pressure at the outlet. Turbulent intensity and hydraulic diameter were the same value of inlet boundary condition.

3.4.4 . Solution methods

Solver settings of the chosen pressure-based solver are as follows. Pressure-velocity coupling refers to the numerical algorithm which uses a combination of continuity and momentum equations to derive an equation for pressure when using the pressure-based solver. Being a robust one, SIMPLE is the default option. Least Square Cell Based is the default gradient interpolation method. It is chosen for being less computationally intensive but having good accuracy. Second order upwind schemes were chosen for energy and momentum equations for 2nd order accuracy [39].

3.4.5 . Convergence criteria

The convergence criteria of 10^{-4} for the residuals of the continuity equation and 10^{-6} for the rest of the residuals were assumed.

4. NUMERICAL ANALYSIS RESULTS

Analyses were run for flat duct geometry and finned duct geometry for various air flow rates. The velocity of air was decided such that turbulence would be enabled in all cases. For this reason, analyses were run for Reynolds numbers of 3000, 5000, 8000 and 10000, in accordance with the parameters described in previous chapter.

In this chapter, results of the analyses are presented. Also, methods for confirming the reliability of analysis are explained in detail. Mesh optimization is done in order to show that number of meshes generated do not have a significant effect on accuracy of the solution. Analysis results are then compared with results obtained from literature. When close resemblance with literature results is obtained, meaning that the duct was simulated close to reality, the analyses are run for all cases.

Mean air and plate temperatures of ducts were observed and plotted, average heat transfer coefficients were calculated, average Nusselt number of ducts, pressure loss through the duct and average Darcy friction factor were plotted against different Reynolds number (flow rates). Two ducts were then compared.

4.1 Results and Validation

Table 4.1 presents the result that would validate the thermal part of the analyses according to equation (2.5). Since the absorber plate dimensions are same for two duct designs, heat supplied is same for all cases. Also since the inlet dimensions are same for two duct designs and air density is taken constant, same mass flow rates for same Reynolds numbers are present for two ducts. Specific heat of air is also taken constant, therefore inlet and outlet temperatures are expected to be same for same Reynolds number. As shown in Table 4.1, this case was confirmed with simulation results.

Analysis software enabled obtaining mean temperatures of air and heat transfer surfaces. By knowing heat transfer areas and using equation (2.5), it is possible to calculate average heat transfer coefficients. Accordingly, heat transfer coefficients were calculated.

Table 4.1 : Some input and output values of numerical analysis

Duct Type	Re	Q_u (W)	\dot{m} (kg/s)	c_p (J/kgK)	T_o (K)	T_i (K)	h (W/m ² K)	A_c (m ²)	T_{pm} (K)	T_{am} (K)
Flat	3000	640	0.012	1006.4	353.8	300	9.6	0.64	421.8	318.1
Flat	5000	640	0.020	1006.4	332.3	300	13.3	0.64	386.0	310.9
Flat	8000	640	0.031	1006.4	320.2	300	18.1	0.64	361.9	306.8
Flat	10000	640	0.039	1006.4	316.2	300	21.2	0.64	352.7	305.5
Finned	3000	640	0.012	1006.4	353.8	300	9.7	1.77	359.1	321.9
Finned	5000	640	0.020	1006.4	332.3	300	13.7	1.77	339.4	313.0
Finned	8000	640	0.031	1006.4	320.2	300	18.7	1.77	327.4	308.1
Finned	10000	640	0.039	1006.4	316.2	300	22.0	1.77	322.9	306.5

As flow velocity increases, average heat transfer coefficient increases as well. Also, average heat transfer coefficients are higher for finned duct. When two ducts are compared according to Table 4.1, it can be seen that finned duct has lower mean plate temperatures and higher air mean temperatures. This indicates that heat supplied is distributed more evenly to air for the case of finned duct.

4.2 CFD Results for Flat Duct

4.2.1 Mesh optimization

Mesh optimization is done in order to determine the optimum number of cells for performing the analyses. The analysis is run consecutively, with increasing number of meshes in each run. For every new analysis finer meshing is developed. This process continues until the change of average Nusselt number and average Darcy friction factor in two consecutive analyses is less than 1%. When this is achieved, it means that solution is independent of meshing and any more refinement of meshing will not improve solution accuracy, but increase computational load. For flat duct geometry, mesh optimization analyses were run for Reynolds number 10000. When number of cells reached 3534000, average Nusselt number differed by 0.5% and average Darcy friction factor differed by 0.3% compared to previous analysis. For 3534000 cells y^+ value was 1.67. This is a good enough value for duct flow heat transfer. This value was lower for smaller Reynolds number. It was decided that 3534000 cells was optimum, and rest of the analyses were run with this grid.

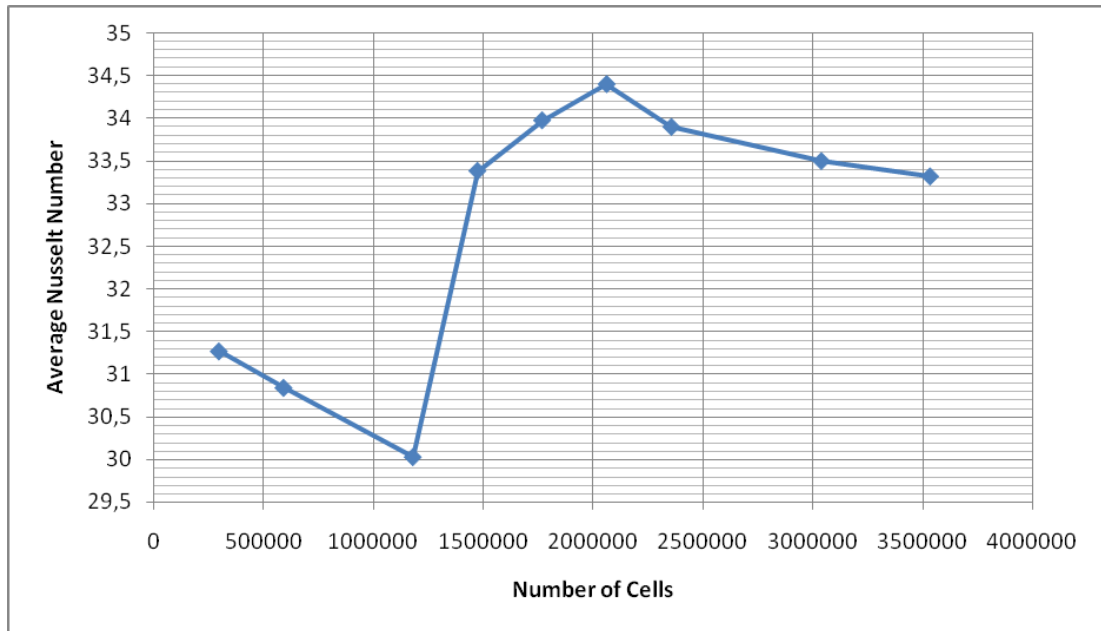


Figure 4.1 : Change of average Nusselt numbers observed with different meshes.

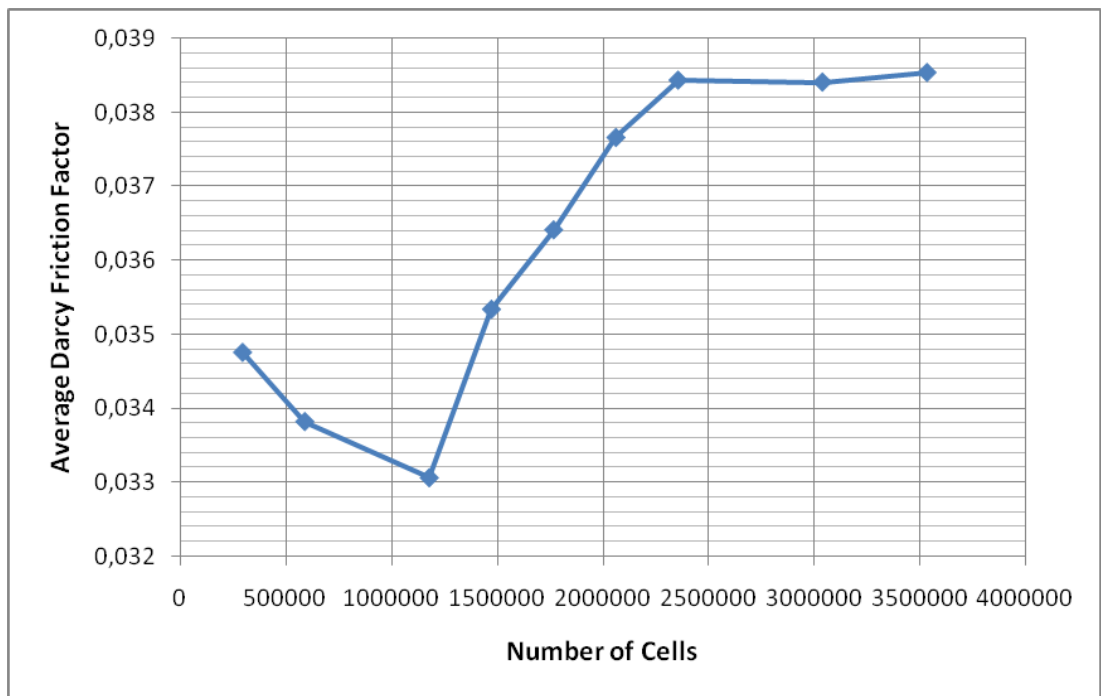


Figure 4.2 : Change of average Darcy friction factors observed with different meshes.

4.2.2 Validation of turbulence model

Results obtained from the analysis were compared with results obtained from literature. A suitable correlation for fully developed turbulent forced convection through a duct with constant properties was determined. Petukhov correlation [42] presented in (4.1) was chosen according to suggestion of Kays and Crawford [43].

$$Nu = \frac{(f/8)RePr}{1,07 + 12,7\sqrt{f/8} (Pr^{2/3} - 1)} \quad (4.1)$$

Friction factors were obtained from Moody's chart. As can be seen from Figure 4.3, results obtained from the analysis were consistent with literature. Therefore, suitability of Standard k- ω turbulence was confirmed and rest of the analyses were run with this model.

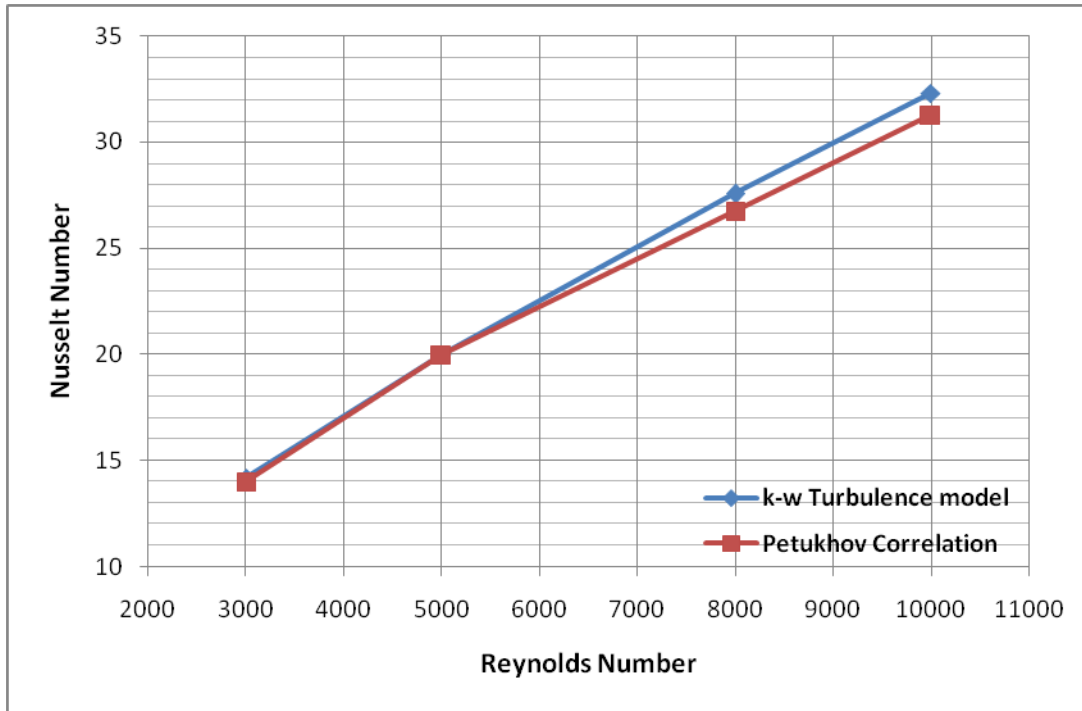


Figure 4.3 : Comparison of analysis results and literature results.

4.2.3 Average Nusselt number

The numerical results regarding average heat transfer characteristics in a flat duct solar air heater are presented in the form of average Nusselt number. In this study Nusselt number has been computed manually using equation (2.9) with heat transfer coefficients obtained from CFD analysis.

As shown in Figure 4.4 average Nusselt numbers calculated for Reynolds number ranging between 3000 and 1000 are plotted against Reynolds number. As the Reynolds number increases, Nusselt number increases as well. This has two reasons. First, high Reynolds number means high mass flow rate, and therefore more fluid is in interaction with the duct absorber surface as Reynolds number increases. Second reason, higher Reynolds number means more turbulence. More turbulence on heat transfer surface results in higher heat transfer coefficients.

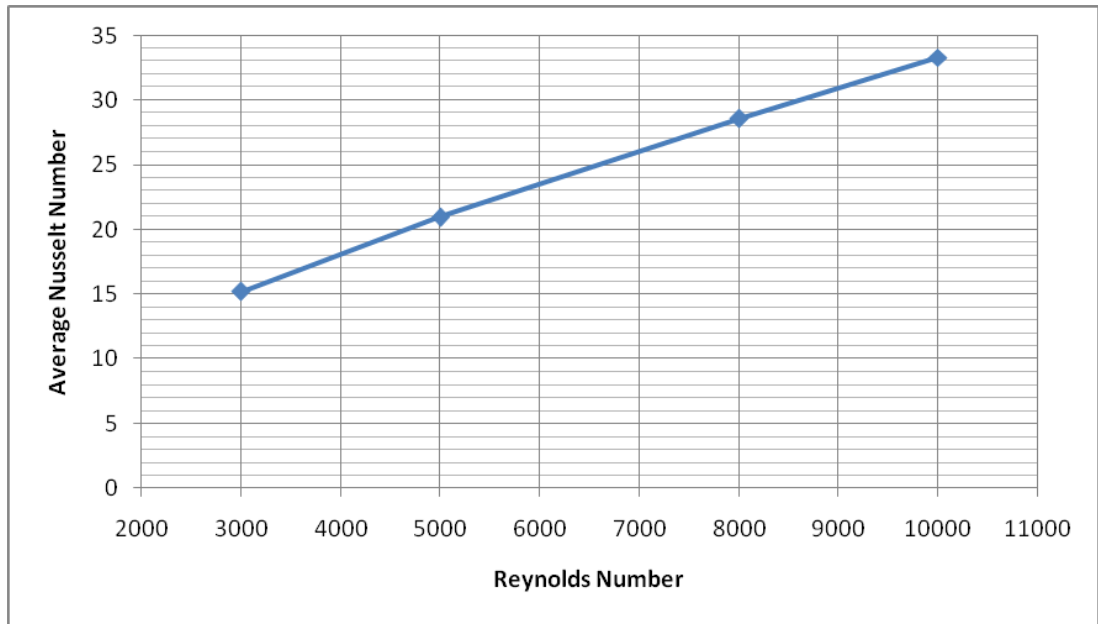


Figure 4.4 : Average Nusselt number vs. Reynolds number.

4.2.4 Pressure loss

The loss through the flat duct is plotted against flow velocity. It can be seen that as the flow velocity increases, pressure loss increases, meaning that more pumping power would be required.

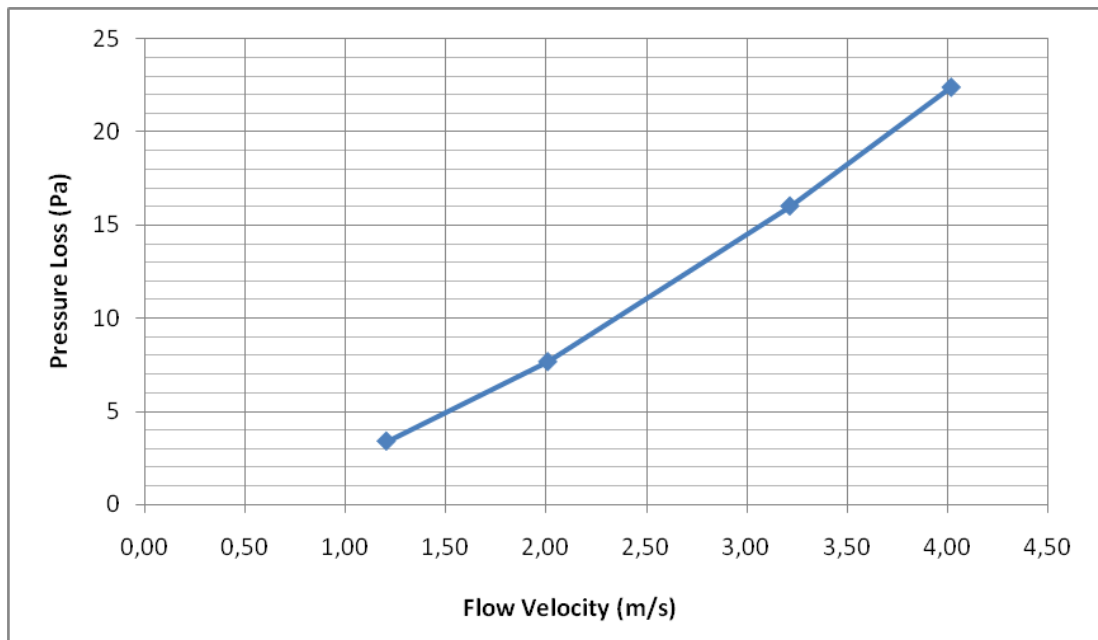


Figure 4.5 : Pressure loss through duct vs. flow velocity.

4.2.5 Average Darcy friction factor

In order to analyze the effect of fluid flow characteristics for flat duct, the values of friction factor are plotted against Reynolds number. Friction factor has been calculated manually, using pressure loss values obtained from CFD model. Unlike Nusselt number, it has been found that the friction factor decreases with increase in Reynolds number. This is due to the effect of velocity in the calculation of friction factor. Same case could be observed in Moody's chart as well.

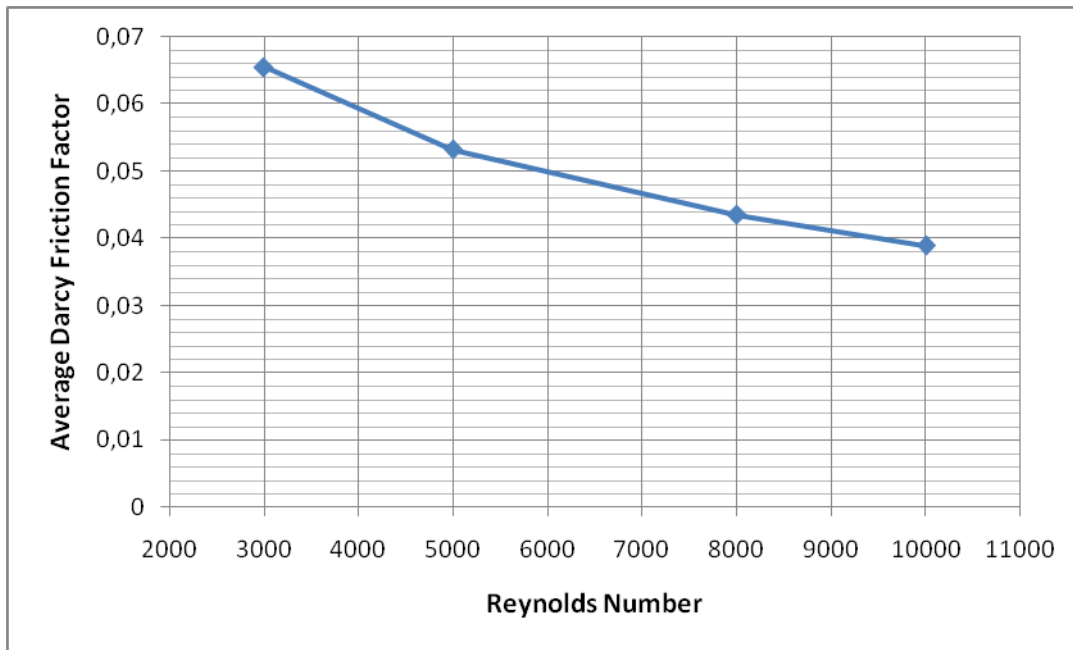


Figure 4.6 : Average Darcy friction factor vs. Reynolds number.

4.3 CFD Results for Finned Duct

4.3.1 Mesh Optimization

For finned duct geometry, mesh optimization analyses were run for Reynolds number 10000 as well. When number of cells reached 7892608, average Nusselt number differed by 0.1% and average Darcy friction factor differed by 0.5% compared to previous analysis. For 7892608 cells y^+ value was 1.93. This is a good enough value for duct flow heat transfer. This value was lower for smaller Reynolds number. It was decided that 7892608 cells was optimum, and rest of the analyses were run with this grid.

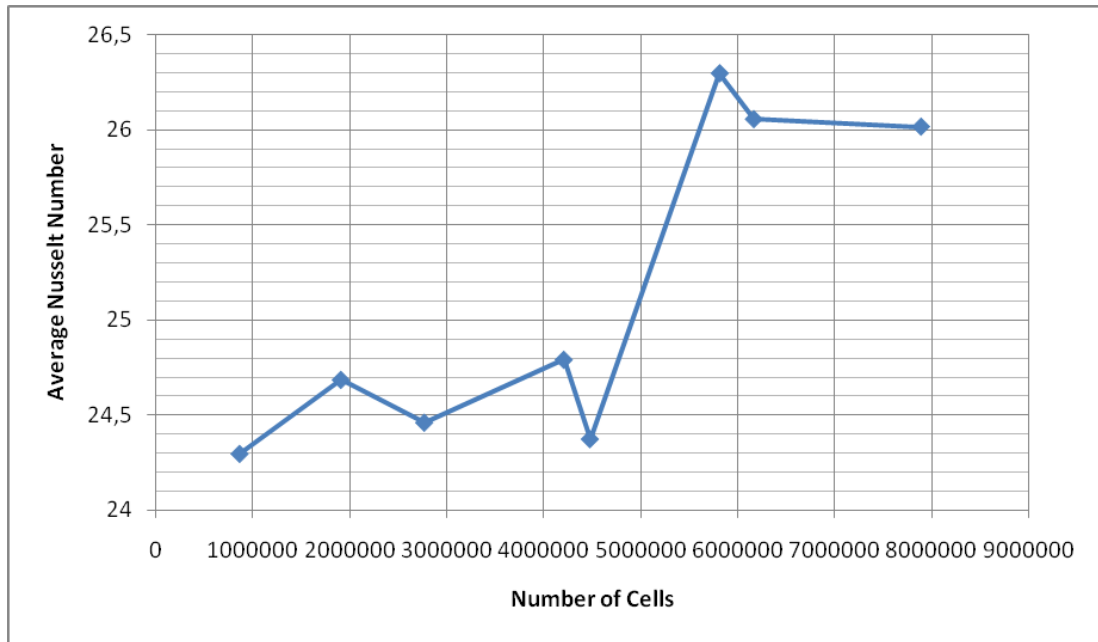


Figure 4.7 : Change of average Nusselt numbers observed with different meshes.

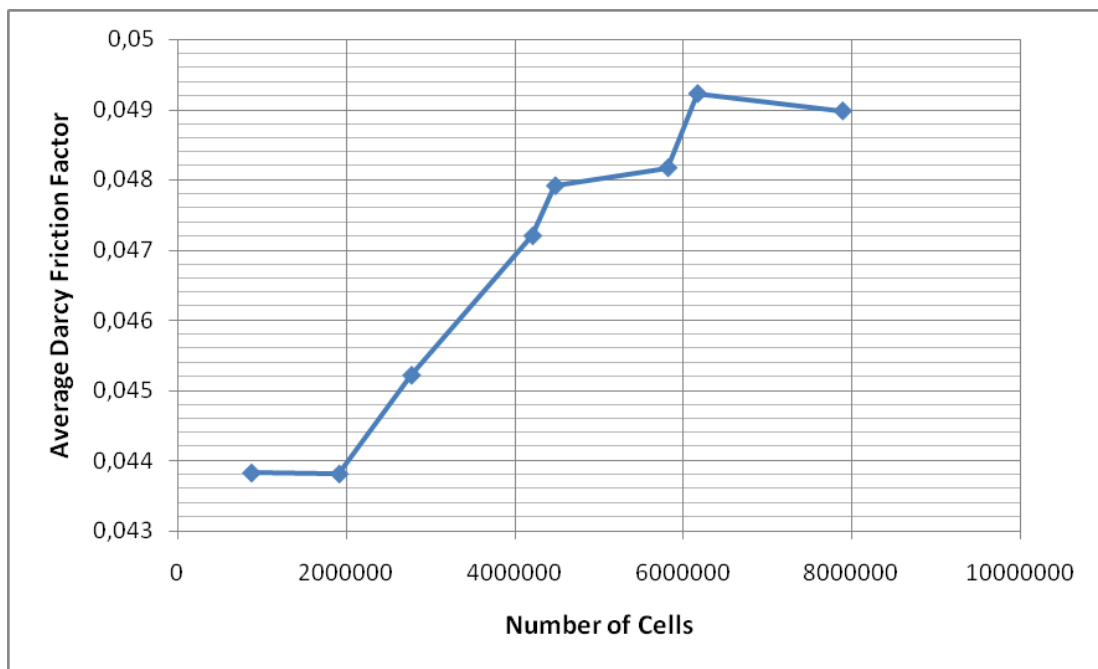


Figure 4.8 : Change of average Darcy friction factors observed with different meshes.

4.3.2 Average Nusselt number

The numerical results regarding average heat transfer characteristics in a finned duct solar air heater are presented in the form of average Nusselt number. In this study Nusselt number has been computed manually using equation (2.9) with heat transfer coefficients obtained from CFD analysis. As shown in Figure 4.9 average Nusselt

numbers computed for Reynolds number ranging between 3000 and 10000 are plotted against Reynolds number. As in the case of flat duct, as the Reynolds number increases, Nusselt number increases as well.

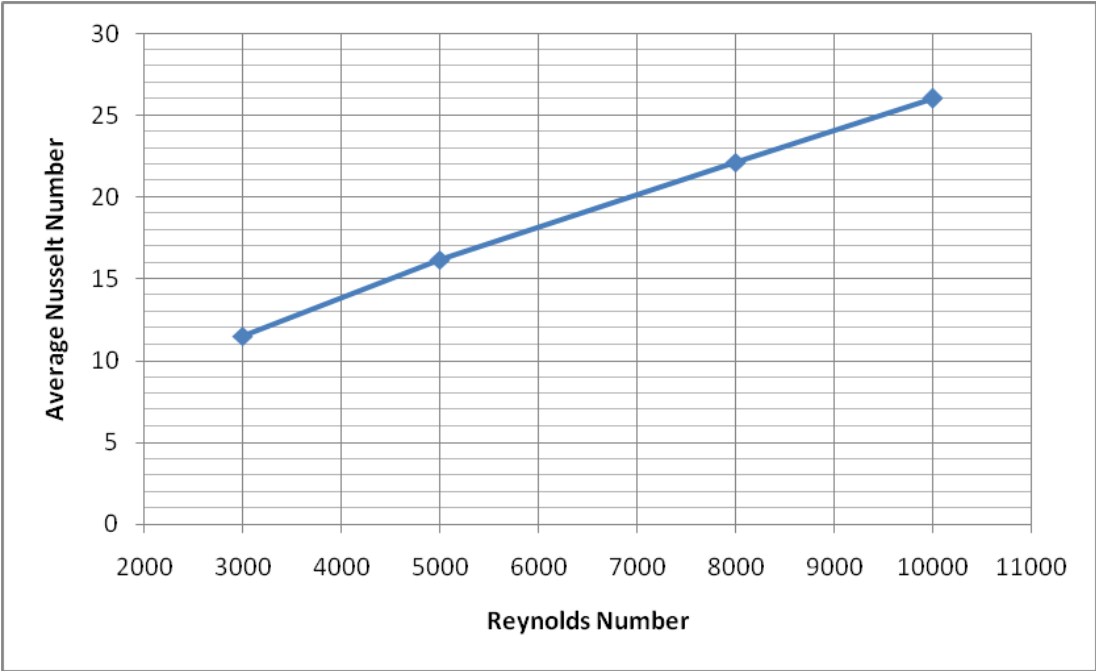


Figure 4.9 : Average Nusselt number vs. Reynolds number.

4.3.3 Pressure loss

The loss through the finned duct is plotted against flow velocity. As in the case of flat duct, it can be seen that as the flow velocity increases, pressure loss increases, meaning that more pumping power would be required.

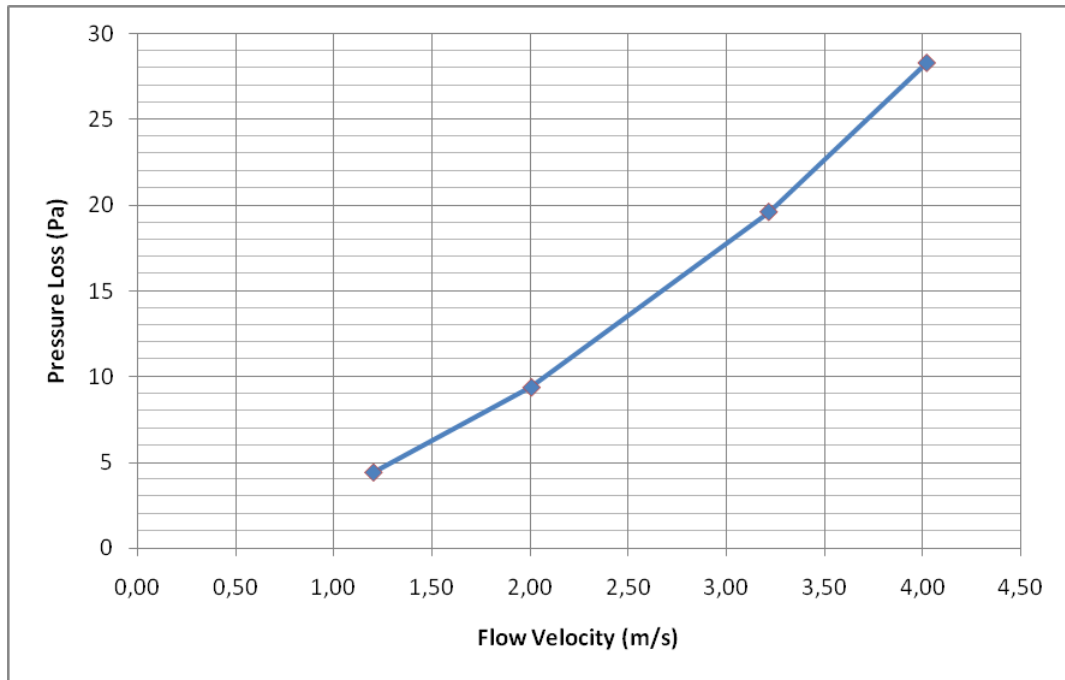


Figure 4.10 : Pressure loss through duct vs. flow velocity.

4.3.4 Average Darcy friction factor

In order to analyze the effect of fluid flow characteristics for finned duct, the values of friction factor are plotted against Reynolds number. Friction factor has been calculated manually, using pressure loss values obtained from CFD model. As in the case of flat duct, friction factor decreases with increasing Reynolds number.

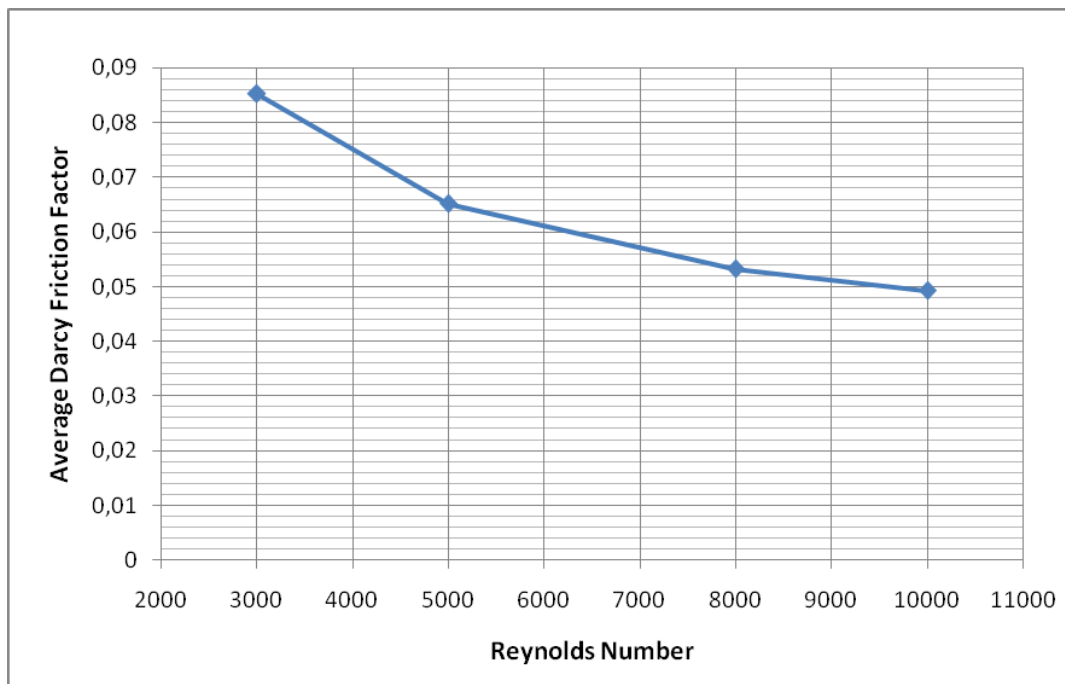


Figure 4.11 : Average Darcy friction factor vs. Reynolds number.

4.4 Comparison of Flat and Finned Duct Types

The flow and heat transfer characteristics get affected in the flow direction with the addition of fins. The aim of this thesis is to observe these effects.

4.4.1 Comparison of mean temperatures

As predicted, since the heat supply, mass flow rates and specific heat of air is same for both cases, temperature difference between the inlet and outlet is exactly same for both designs. As shown in Figure 4.12, increase in temperature becomes less as the flow velocity increases.

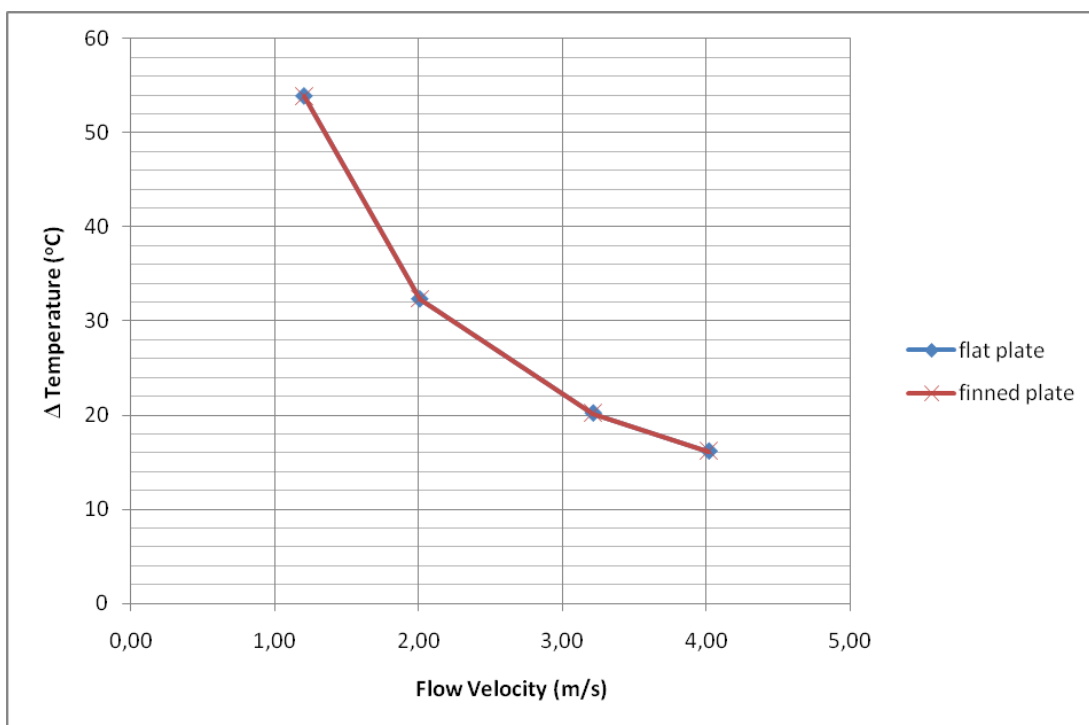


Figure 4.12 : Temperature difference between inlet and outlet.

Figure 4.13 shows the mean plate temperatures and mean air temperatures for all cases. Again, as the flow velocity increases all temperatures decrease. The main conclusion that can be drawn from this figure is that the differences between mean plate temperatures and mean air temperatures are significantly higher for flat duct. This means that for finned duct heat transfer from absorber plate to air is better. Also, mean air temperatures are higher for flat duct. For flat duct, excessive heating of absorber plate causes inefficiency. When heat transfer areas are taken into account, higher average heat transfer coefficients are calculated for finned duct.

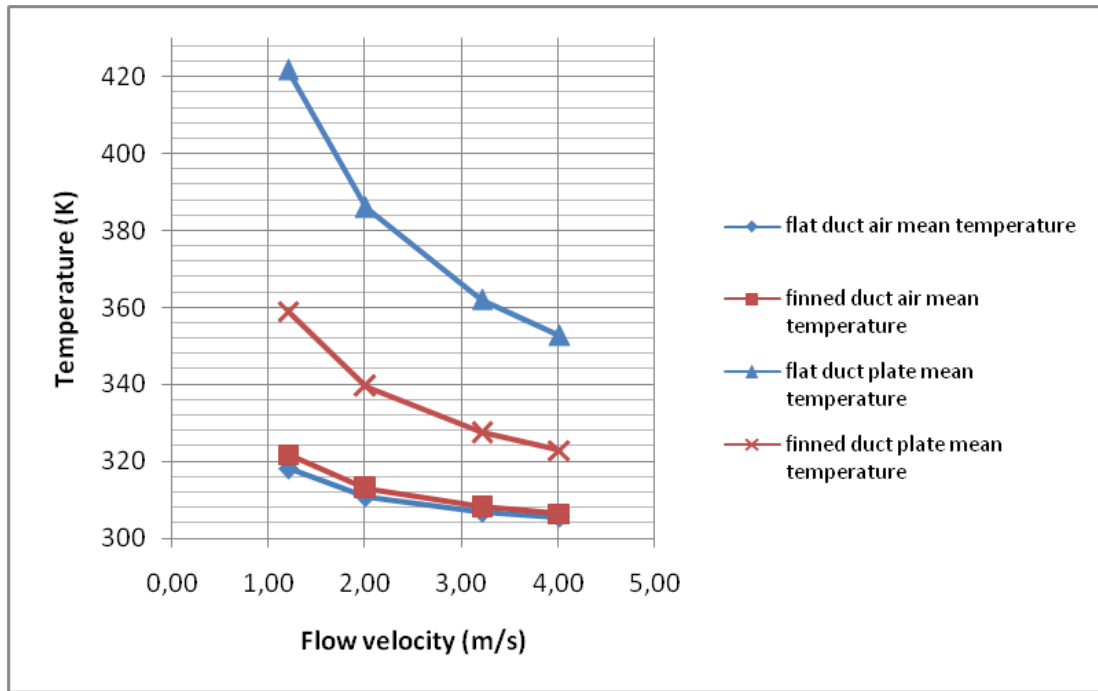


Figure 4.13 : Mean plate and mean air temperature comparison of two ducts.

This case can be visualized with images obtained from ANSYS Fluent results as shown in Figures 4.14, 4.15, 4.16 and 4.17. These figures show the temperature contours of absorber plates and outlets of two duct designs. It can be seen that with addition of fins, temperature gradients of air and heat transfer surfaces became smaller. While the maximum temperature reached around 500 K on flat absorber plate, it reached around 380 K on finned absorber plate. The heat distribution occurs more evenly for finned duct, and this is desirable. The outlet views show that for flat duct, air close to absorber plate is extremely hot compared to air far from absorber plate. Whereas for finned duct, temperature gradients are not as extreme. In practice smaller temperature gradients obtained from finned design is more desirable.

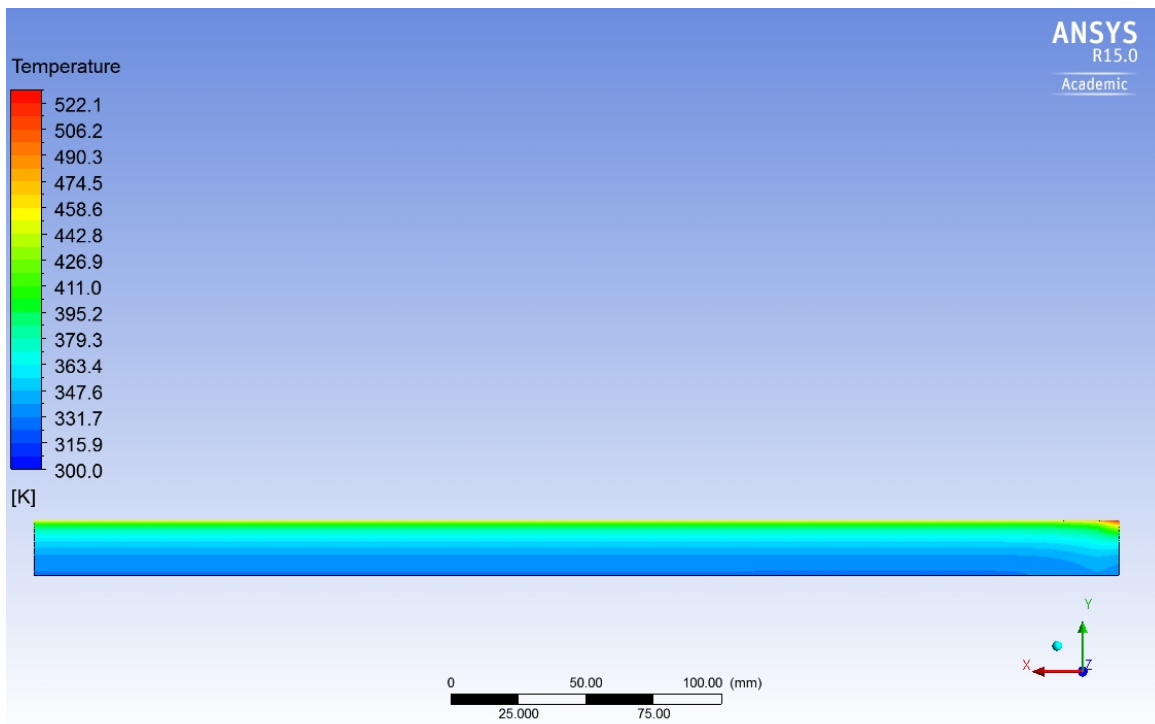


Figure 4.14 : Cross section view of flat duct outlet when $Re = 3000$.

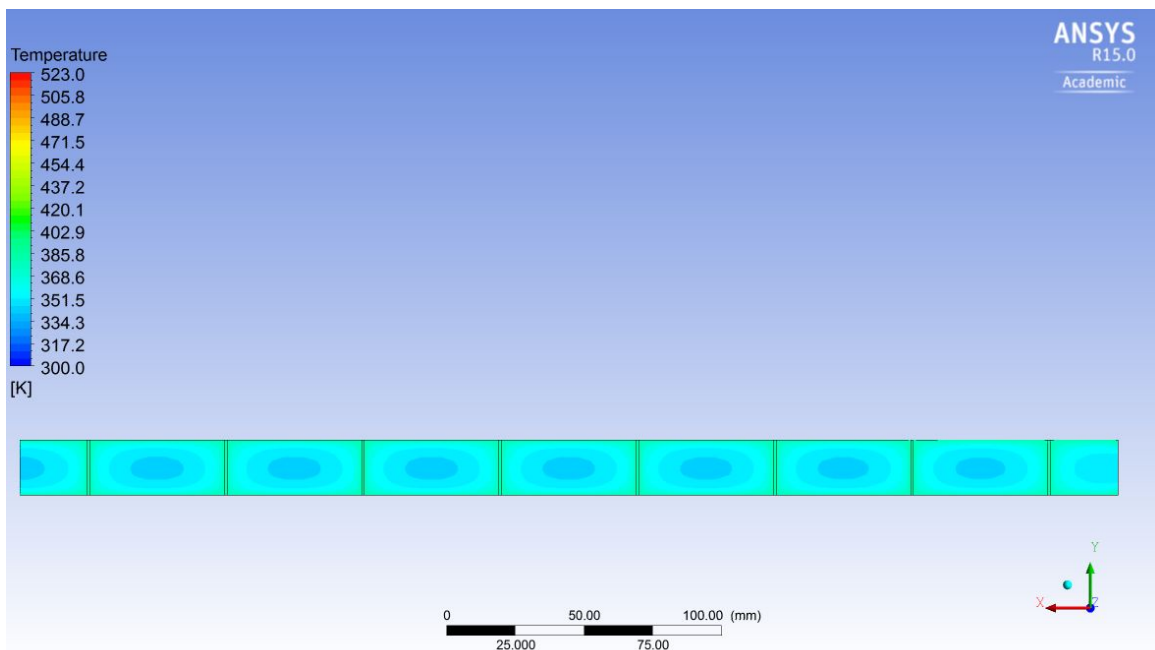


Figure 4.15 : Cross section view of finned duct outlet when $Re = 3000$.

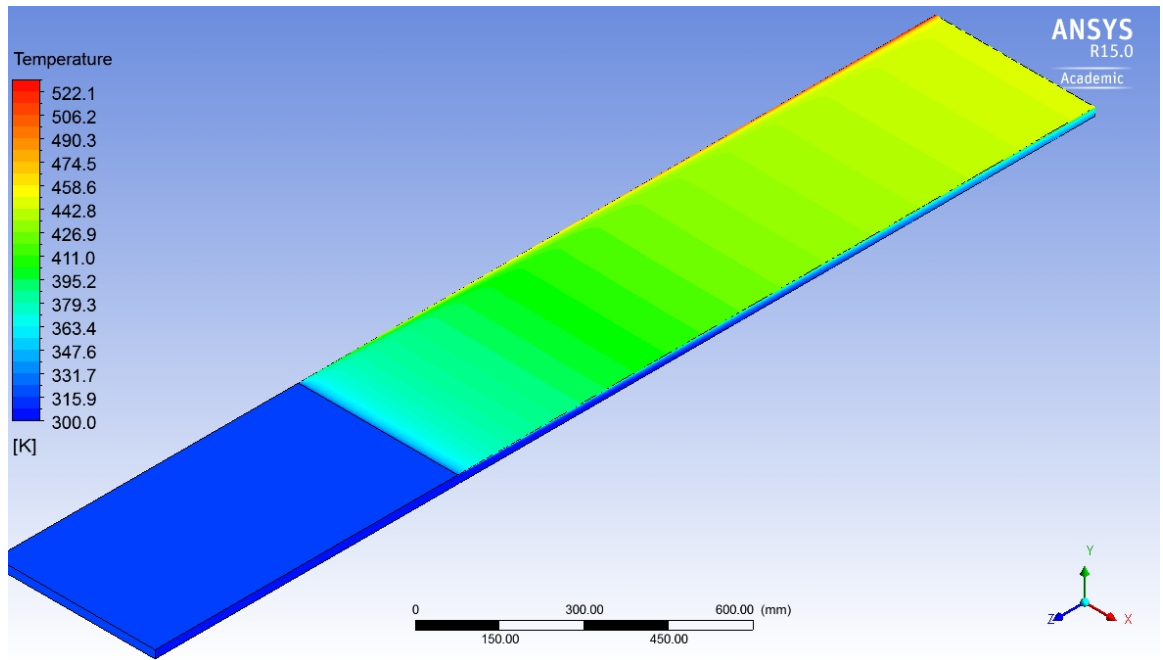


Figure 4.16 : Isometric view of entry section and absorber plate of flat duct when $Re=3000$.

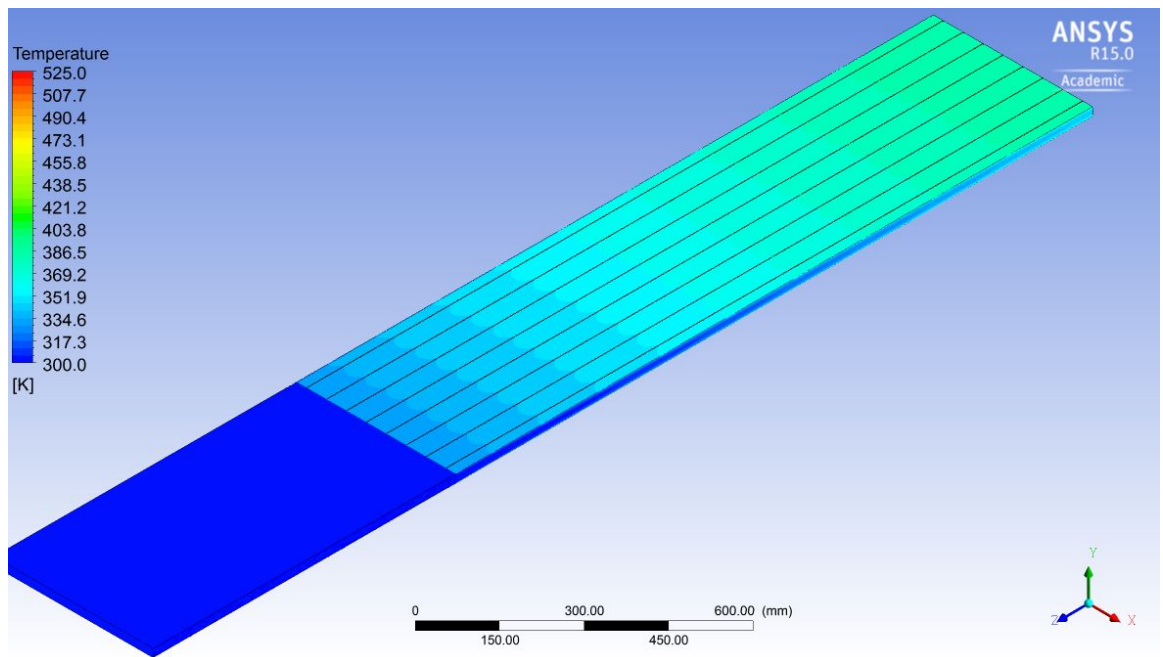


Figure 4.17 : Isometric view of entry section and absorber plate of finned duct $Re=3000$.

4.4.2 Comparison of average Nusselt numbers

Although the propagation of heat was better for finned duct design and although higher average heat transfer coefficients were obtained, the average Nusselt number was found less for finned duct. The reason is, due to addition of fins, heat transfer occurs in smaller channels with smaller hydraulic diameters. As a result, smaller Nusselt numbers are obtained. In other words, the Nusselt number was less for finned ducts because with the change in flow characteristics of air due to fins, decrease in the turbulent intensity occurred caused by decrease in turbulent dissipation rate and turbulent kinetic energy.

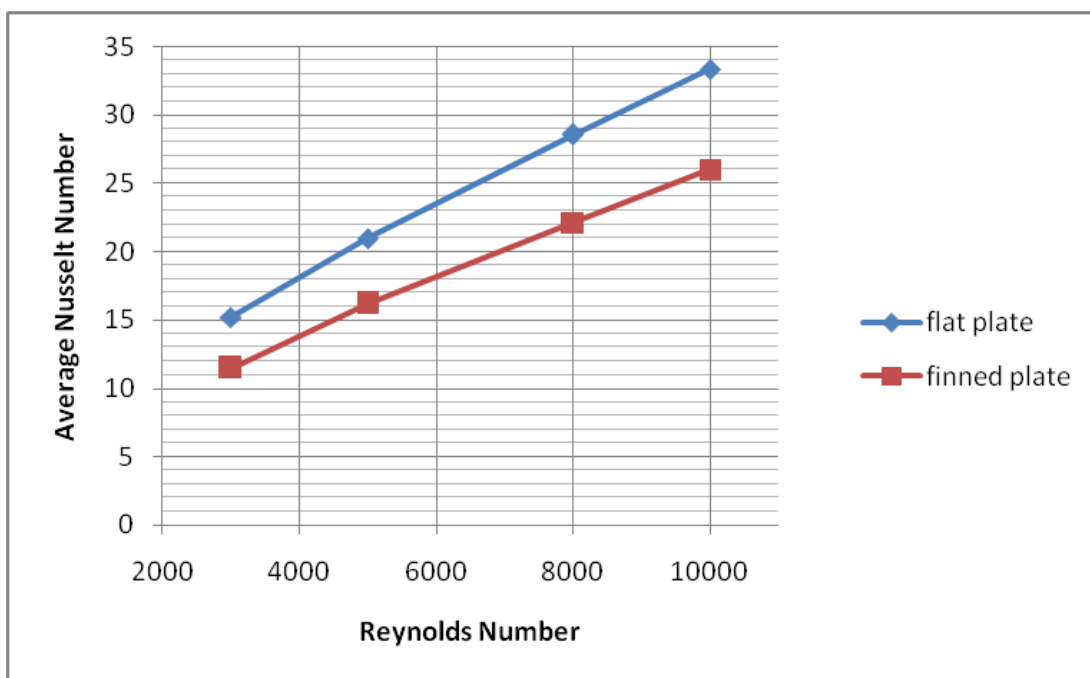


Figure 4.18 : Average Nusselt number comparison of two ducts.

4.4.3 Comparison of pressure losses

More pressure loss was observed for finned duct. This is because fins acted as obstacles for air flow. Amount of friction force that air had to overcome was higher since the air – heat transfer surface interaction area was higher. Difference in pressure losses for two duct types increases with increasing flow rates. This is due to increase in turbulence.

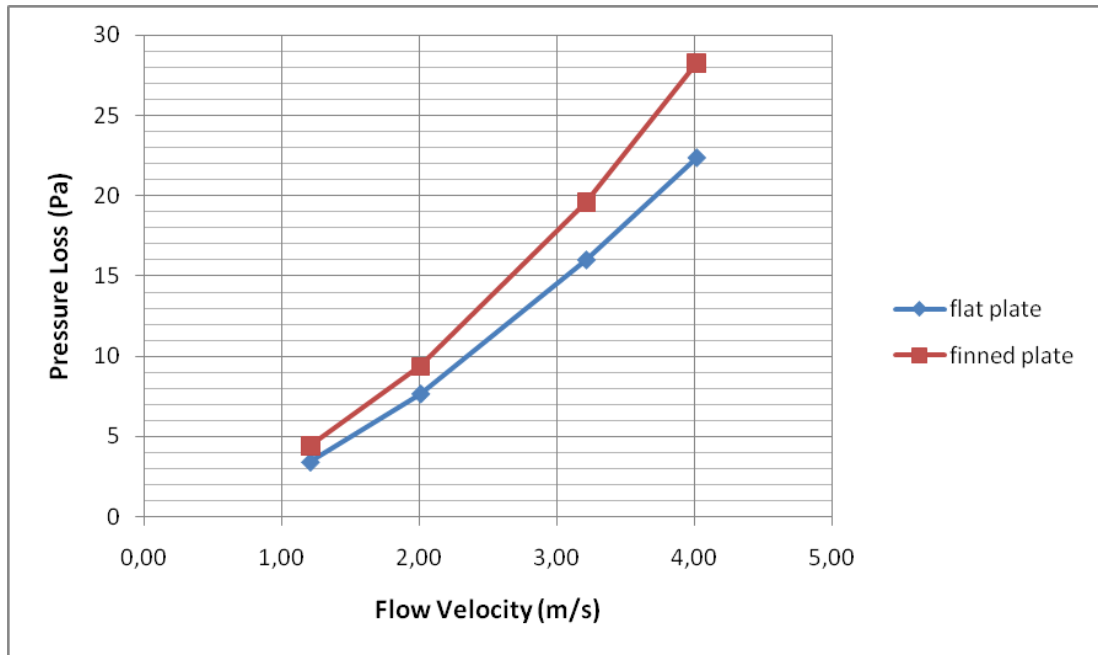


Figure 4.19 : Pressure loss comparison of two ducts

4.4.4 Comparison of average Darcy friction factors

As a result of increase in pressure loss, the average friction factor is enhanced by the presence of fins compared to a flat duct of a solar air heater. The flow blockage due to the presence of fins is a dynamic factor to cause a high pressure drop.

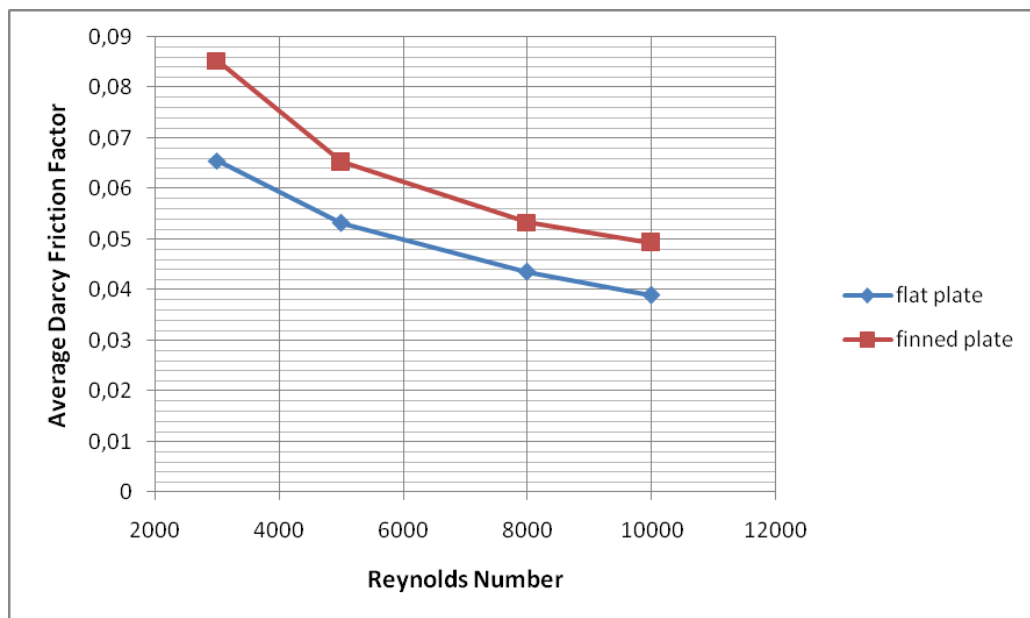


Figure 4.20 : Average Darcy friction factor comparison of two ducts.

4.5 Thermo - Hydraulic Performance of Finned Ducts

Thermo - hydraulic performance parameter is defined as overall enhancement ratio and represented by (4.2). A design that yields the value of this parameter greater than one is considered successful. Higher the value of this parameter, better is the performance of the solar air heater.

$$\text{Overall Enhancement Ratio} = \frac{Nu_{finned} / Nu_{flat}}{(f_{finned} / f_{flat})^{1/3}} \quad (4.2)$$

According to results obtained from analyzes, Nusselt number decreases and friction factor increases with addition of fins. The calculated enhancement ratios for each Reynolds number is presented in Table 4.2.

Table 4.2 : Overall enhancement ratios for each Reynolds number.

Reynolds Number	Overall Enhancement Ratio
3000	0.692
5000	0.722
8000	0.724
10000	0.722

The enhancement in the collector performance due to addition of obstacles may be evaluated on the basis of thermo - hydraulic performance parameter which incorporates both the thermal as well as hydraulic considerations. From this point of view, although addition of fins has obvious positive outcomes, the duct design with fins is thermo – hydraulically less efficient than a flat duct. This is mainly due to reduction of turbulence that occurred with the addition of fins.

5. CONCLUSIONS AND RECOMMENDATIONS

In this thesis, two different duct designs for solar air collectors were studied in within the frame of thermal and hydrodynamic properties. There are many factors affecting the efficiency of a solar air collector. Interaction of air and heat transfer surfaces is one of these factors. The aim of the study was to propose a new duct design for performance improvement and to compare the proposed design and conventional design by using numerical methods, utilizing Computational Fluid Dynamics software.

A flat, rectangular duct with a 20mm x 800mm cross section was determined as the conventional design. In the proposed design, fins of 1mm thickness were placed under the absorber plate and they had 50mm between each other. The ducts were modeled in three dimensions. Depth of the duct was 2360mm, 760mm being the entrance region and 1600mm being the absorber plate. Length of entrance length was determined according to ASHRAE Standard 93-2010. It was placed in the simulation in order to achieve fully developed flow below absorber plate.

Modeling and numerical analysis of the duct were done in ANSYS Fluent software. Finite volume method was used. Forced convection heat transfer and turbulent, three dimensional, fully developed flow was considered. Air was chosen as the working fluid and was assumed to be incompressible for range of analysis since variation in density is very small. Aluminum was chosen as the material of duct components and was assumed homogeneous, isotropic and having constant thermal conductivity. By only modeling the duct and air flowing through, radiation or convection losses to environment were ignored.

Analyses were run for two different ducts separately, with 1000W/m^2 constant heat flux boundary condition applied on absorber plate and with different Reynolds numbers ranging from 3000 to 10000. To save computational power and time, only half of the ducts were modeled since the ducts were symmetric with respect to direction of flow. Before starting analyses, mesh optimization was done in order to obtain results that were independent from meshing of the geometry. Also, by

comparing results of flat duct with literature, Standard $k-\omega$ turbulence model was found to give accurate results. Therefore, this model was employed for the rest of the analyses.

The boundary conditions were defined for every part of duct. Inlet of the duct was defined as velocity boundary condition. Inlet velocities were determined according to chosen Reynolds numbers. Air entrance temperature was 300K. Outlet of the duct was defined as pressure boundary condition. It was assumed that the outlet pressure was same as atmospheric pressure. On absorber plate, constant heat flux was applied. Rest of the surfaces were adiabatic. No-slip boundary condition was applied on all walls.

With above specifications, analyses were run for two duct types. Mean air and plate temperatures and pressure loss through duct were recorded. Average Nusselt number and average Darcy friction factor were calculated. Results were presented with graphs in chapter 4. Two duct types were compared.

For both analyses, the following statements were common. According to results for fully developed turbulent flows, amount of heat transfer increases with increasing Reynolds number. Higher Nusselt numbers are observed. Faster flows, meaning higher Reynolds numbers results in more turbulence and as a result heat transfer coefficient between the surface and fluid increases. However for higher Reynolds number, meaning higher mass flow rates, smaller outlet temperatures are observed. Although the heat transfer performance is better, same amount of heat is used for heating more air, therefore the temperature change becomes less. At the same time for faster flows, pressure loss through the duct increases and Darcy friction factor decreases. This is due to increasing effects of turbulence.

When the results of different designs were compared, thanks to CFD software, it was possible to visualize the simulations. It was observed that with additions of fins, heat distribution became better. For flat duct, higher absorber plate mean temperatures and lower air mean temperatures were observed compared to finned duct. For finned duct, absorber plate mean temperature was lower because heat transfer via conduction occurred from top of the fin to bottom of the fin. As a result, air flowing close to bottom plate could be heated from the fins and the back plate. For flat duct,

only air flowing close to absorber plate could be heated and high temperature gradients were observed at outlet.

Amount of pressure drop increased with addition of fins. This means, more energy is required to force the fluid to flow. In other words, higher pumping power would be necessary for the operation of a finned duct.

When Nusselt number and Darcy friction factor values obtained from analysis were compared, it was observed that flat plate duct had higher Nusselt number and lower friction factor values compared to finned duct. This resulted in overall enhancement ratios less than one for finned duct. This means that the proposed design is unfavorable from thermo-hydraulic performance point of view. Normally, addition of roughness elements such as fins would increase turbulence, therefore increase heat transfer coefficient and Nusselt number. However, in the proposed design fins created smaller ducts with smaller hydraulic diameters that had decreased turbulence effects, therefore lower Nusselt numbers were obtained for same Reynolds number when compared with flat duct, even though the average heat transfer coefficient were higher for finned duct. At the same time, with increase in heat transfer area and better heat distribution, higher mean air temperatures were observed.

In the proposed finned design, fins were compressed between the absorber plate and back plate to achieve ease of construction and avoid welding costs. Although thermo-hydraulically not favorable, proposed design enables better heat distribution, higher air mean temperatures and higher average heat transfer coefficients. If the air compressor supplying air to this duct were to run with free solar energy, then this design would be feasible. Further experimental and economical studies could be made for this design. Material and building cost analysis and real life transient performance analysis would enrich the results of this study.

REFERENCES

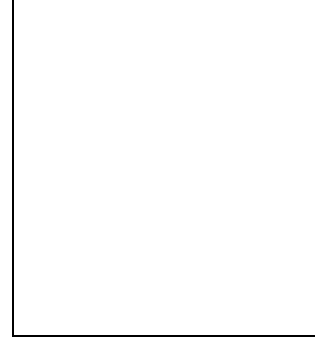
- [1] **Kreith, F., and Kreider, J.F.** (1978). Principles of Solar Engineering, McGraw-Hill, New York, USA
- [2] **Kalogirou, S.A.**(2004).Solar Thermal Collectors and Applications.*Progress in Energy and Combustion Science* 30(2004) pp. 231-295
- [3] **Url-1**<<http://lightontheearth.blogspot.com.tr/p/homeowners-solar-manual-online.html>> , date retrieved 27.09.2015
- [4] **Selçuk, K.** (1974). Solar Air Heaters and Their Applications.*Solar Energy Engineering*, pp. 155-182
- [5] **Charters, W.W.S., and Macdonald, R.W.G.**(1982). Solar Air Heating: Technology and Applications. *First U.S.–China Conference on Energy, Resources and Environment*, 7–12 November 1982, Beijing, China. pp. 464-471
- [6] **Close, D.J.**(1963). Solar Air Heaters for Low and Moderate Temperature Applications, *Solar Energy Vol.7 Issue 3*, pp. 117-124.
- [7] **Whillier, A.**(1964). Performance of Black-Painted Solar Air Heaters of Conventional Design, *Solar Energy Vol.8 Issue 1*, pp. 31-37.
- [8] **Kuzay, T.M., Malik, M.A.S., and Boer, K. W.**(1974). Solar collectors of solar one, Proceedings of the NSF/RANN Workshop on Solar Collectors for Heating and Cooling of Buildings, New York.
- [9] **Malik, M.A.S., and Buelow, F.H.**(1973).Heat Transfer Characteristics of a Solar Dryer, International Congress on the Sun in the Service of Mankind, Paris.
- [10] **Hollands, K.G.T., and Shewen, E.C.**(1981).Optimization of Flow Passage Geometry for Air Heating Plate-Type Solar Collectors, *Journal of Solar Energy Engineering Vol.103*, pp.323-330.
- [11] **Bhargava, A.K., Garg, H.P., and Sharma V.K.**(1982). Evaluation of the Performance of Air Heaters of Conventional Designs, *Solar Energy Vol.29 Issue 6*, pp. 523-533.
- [12] **Garg, H.P., Datta, G., and Bandyopadhyay,B.**(1983). A Study on the Effect of Enhanced Heat Transfer Area in Solar Air Heaters, *Energy Conversion and Management, Vol.23 Issue 1*, pp. 43-49.
- [13] **Bhargava, A.K., Fumagalli, S., Rizzi, G., Frascione, A., Ruspini, G., and Mahajan, S.**(1986). A Comparative Experimental Study of a Two Pass Solar Air Heater with Conventional Designs, *Proceedings of the Ninth Biennial Congress of the International Solar Energy Society, Intersol Eighty Five*, pp. 161-165.

- [14] **Hegazy, A.A.**(1996). Optimization of Flow Channel Depth for Conventional Flat Plate Solar Air Heaters, *Renewable Energy*, Vol. 7, No.1, pp.15-21.
- [15] **Hegazy, A.A.**(1999). Optimum Channel Geometry for Solar Air Heaters of Conventional Design and Constant Flow Operation, *Energy Conservation & Management Vol.40 Issue 8*, pp. 757-774.
- [16] **Hegazy, A.A.**(2000). Performance of Flat Plate Solar Air Heaters with Optimum Channel Geometry for Constant / Variable Flow, *Energy Conversion and Management*, Vol.41 Issue 4, pp.401-417.
- [17] **Choudhury, P.M., Chauhan, P.M., and Garg, H.P.**(1995). Design Curves for Conventional Solar Air Heaters, *Renewable Energy*, Vol.6 , No.7, pp.739-749.
- [18] **Metwally M.N., Abou-Ziyan, H.Z., and El-Leathy, A.M.**(1997). Performance of Advanced Corrugated-Duct Solar Air Collector Compared with Five Conventional Designs, *Renewable Energy*, Vol. 10, No.4, pp.519-537.
- [19] **Kabeel, A.E., and Mecerik, K.,**(1998). Shape Optimization for Absorber Plates of Solar Air Collector, *Renewable Energy*, Vol. 13, Issue 1, pp. 121–131.
- [20] **Ammari, H.D.**(2003). A Mathematical Model of Thermal Performance of a Solar Air Heater with Slats, *Renewable Energy*, Vol.28, pp.1597–1615.
- [21] **Karim, M.A., and Hawlader, M.N.A.**(2004).Development of Solar Air Collectors for Drying Applications, *Energy Conversion and Management*, Vol. 45, Issue 3, pp. 329–344.
- [22] **Karim, M.A., and Hawlader, M.N.A.**(2006).Performance Evaluation of a V-Groove Solar Air Collector for Drying Applications, *Applied Thermal Engineering Vol.26, No.1*, pp.121-130.
- [23] **Aharwal, K.W., Gandhi,B.K., and Saini, J.S.**(2008). Experimental Investigation on Heat-transfer Enhancement due to a Gap in an Inclined Continuous Rib Arrangement in a Rectangular Duct of Solar Air Heater, *Renewable Energy Vol.33*, pp. 585–596.
- [24] **Karakaya, H., and Durmuş, A.**(2009).Farklı Tip YüzeyGeometrilerineSahipHavalıKolektörlerdeVerimveEkserjiAnalizi, V. YeniveYenilenebilirEnerjiKaynaklarıSempozyumu, TMMOB MakineMühendisleriOdası Kayseri Şubesi, Kayseri, pp.182-192.
- [25] **Kumar, T.S., Thakur, N.S., Kumar, A., and Mittal,V.**(2010). Use of Artificial Roughness to Enhance Heat Transfer in Solar Air Heaters - A Review, *Journal of Energy in Southern Africa*, Vol.21, No.1, pp.35-51
- [26] **El-Sebai,A.A., Aboul-Enein,S., Ramadan, M.R.I, Shalaby, S.M., and Moharram, B.M.**(2011). Thermal Performance Investigation of Double Pass Finned Plate Solar Air Heater, *Applied Energy*, Vol. 88, pp. 1727–1739

- [27] **Ingle, P.W., Pawar, A.A., Deshmukh, B.D., and Bhosale, K.C.**(2013). CFD Analysis of Solar Flat Plate Collector, *International Journal of Emerging Technology and Advanced Engineering*, Vol.3, Issue 4, pp.337-342
- [28] **Chaudhari, S., Makwana, M., Choksi, R., and Patel, G.**(2014). CFD Analysis of Solar Air Heater, *International Journal of Engineering Research and Applications*, Vol.4, Issue 6, pp. 47-50.
- [29] **Amraoui.M.A., and Aliane.K.**(2014). Numerical Analysis of a Three Dimensional Fluid Flow in a Flat Plate Solar Collector, *International Journal of Renewable and Sustainable Energy*, Vol.3, No.3, pp.68-75.
- [30] **Yadav, A.S., and Bhagoria, J.L.**(2013). Heat Transfer and Fluid Flow Analysis of Solar Air Heater- A Review of CFD Approach, *Renewable and Sustainable Energy Reviews*, Vol.23, pp. 60-79.
- [31] **Chaube, A., Sahoo, P.K., and Polanski, S.C.**(2006). Effect of Roughness Shape on Heat Transfer and Flow Friction Characteristics of Solar Air Heater with Roughened Absorber Plate, *WIT Transactions on Engineering Sciences*, Vol.53, pp. 43-51.
- [32] **Kumar, S., and Saini, R.P.,**(2009).CFD Based Performance Analysis of a Solar Air Heater Duct Provided with Artificial Roughness, *Renewable Energy*, Vol.34, pp.1285-1291.
- [33] **Nayak, S.P., Shukla, P., and Ghodke, S.**(2012). Heat Transfer Analysis of Rectangular Roughness Rib in Solar Air Heater Duct by CFD, *International Journal of Advanced Research in Science, Engineering and Technology*. Vol.1, Issue 3, pp. 25-30.
- [34] **Yadav, A.S., and Bhagoria, J.L.**(2013). A CFD Based Heat and Fluid Flow Analysis of a Solar Air Heater Provided with Circular Transverse Wire Rib Roughness on the Absorber Plate, *Energy*, Vol.55, pp.1127-1142.
- [35] **Yadav, A.S., and Bhagoria, J.L.**(2014). A CFD Based Thermo-Hydraulic Performance Analysis of an Artificially Roughened Solar Air Heater Having Equilateral Triangular Sectioned Rib Roughness on the Absorber Plate, *International Journal of Heat and Mass Transfer*, Vol.70, pp. 1016-1039.
- [36] **Ong, K.S.** (1995). Thermal Performance of Solar Air Heaters: Mathematical Model and Solution Procedure, *Solar Energy* Vol.55, No.2, pp.93-109
- [37] **Bergman, T.L., Lavine, A.S., Incropera, F.P., DeWitt, D.P.** (2011).Introduction to Heat Transfer, 6th Ed., John Wiley&Sons, Inc., USA.
- [38] **Url-2**<https://en.wikipedia.org/wiki/Moody_chart> , date retrieved 24.10.2015
- [39] **Lee C.K., Abdel-Moneim S.A.** (2001). Computational Analysis of Heat Transfer in Turbulent Flow Past a Horizontal Surface with 2-D, *IntCommun. Heat Mass Transfer*, Vol. 28 No.2, pp. 161-170.
- [40] **ANSYS.** (2010). Customer Training Material

- [41] **ASHRAE STANDARD 93-2010**.(2010). Methods of Testing to Determine the Thermal Performance of Solar Collectors.*ASHRAE*.
- [42] **Petukhov, B.S.** (1970). Heat Transfer and Friction in Turbulent Pipe Flow with Variable Physical Properties,*Advances in Heat Transfer*. New York: Academic Press
- [43] **Kays, W.M., Crawford, M.E.** (1993). Convective Heat and Mass Transfer, 3rd Ed. New York: McGraw-Hill

CURRICULUM VITAE



Name Surname: Cem Çorapçiođlu

Place and Date of Birth: 30.11.1988

E-Mail: corcem@gmail.com

EDUCATION:

B.Sc.: 2012, Bođaziçi University, Faculty of Engineering,
Mechanical Engineering